

In presenting the dissertation as a partial fulfillment of the requirements for an advanced degree from the Georgia Institute of Technology, I agree that the Library of the Institute shall make it available for inspection and circulation in accordance with its regulations governing materials of this type. I agree that permission to copy from, or to publish from, this dissertation may be granted by the professor under whose direction it was written, or, in his absence, by the Dean of the Graduate Division when such copying or publication is solely for scholarly purposes and does not involve potential financial gain. It is understood that any copying from, or publication of, this dissertation which involves potential financial gain will not be allowed without written permission.

*Handwritten signature*

3/17/65  
b

FIRST ORDER GREEN FUNCTION  
THEORY OF THE  
HEISENBERG FERROMAGNET

A THESIS

Presented to

The Faculty of the Graduate Division

by

John Alexander Copeland, III

In Partial Fulfillment

of the Requirements for the Degree


Doctor of Philosophy in the School of Physics


Georgia Institute of Technology

June, 1965

FIRST ORDER GREEN FUNCTION THEORY  
OF THE HEISENBERG FERROMAGNET

Approved:

  
\_\_\_\_\_  
Dr. H. A. Gersch, Chairman

  
\_\_\_\_\_  
Dr. V. D. Crawford

  
\_\_\_\_\_  
Dr. J. C. Currie

Date approved by Chairman:

  
\_\_\_\_\_  
28 May 1965

## ACKNOWLEDGMENTS

I would like to thank Dr. Harold A. Gersch for suggesting the thesis problem and for his guidance and encouragement during the course of the research. I would also like to thank Dr. Edwin J. Scheibner and Dr. Vernon D. Crawford for their counseling throughout my career as a student of physics and my wife, Sandra, for the moral support she has given me.

This work has been supported in part by the U. S. Atomic Energy Commission under the Metallurgy and Materials Program of the Division of Research. Participation in the project "Surface Properties of Magnetic Materials" directed by Dr. Scheibner of the Georgia Institute of Technology School of Physics was responsible for my initial interest in magnetism. Experience in other phases of this project have been a valuable supplement to the theoretical work of this thesis.

I would also like to thank Mrs. Betty Jaffe for the extraordinary care she took in typing the thesis.

Permission was granted by the Graduate Division to follow the standard form of the American Institute of Physics in using the explanatory captions under the figures in the text. The proper titles appear in the "List of Illustrations."

## TABLE OF CONTENTS

	Page
ACKNOWLEDGMENTS	ii
LIST OF TABLES . . . . .	iv
LIST OF ILLUSTRATIONS . . . . .	v
Chapter	
I. INTRODUCTION . . . . .	1
The Weiss Molecular Field	
The Heisenberg Ferromagnet	
Temperature Dependent Green Functions	
II. REVIEW OF GREEN FUNCTION THEORY . . . . .	12
Properties of Green Functions	
Green Function for the Heisenberg Ferromagnet	
Extension to $S > 1/2$	
III. CALCULATIONAL PROCEDURE . . . . .	36
IV. BEHAVIOR WHEN MAGNETIZATION VANISHES . . . . .	42
V. CHOOSING THE TERMINATION FUNCTION . . . . .	51
VI. GENERAL RESULTS . . . . .	60
VII. CONCLUSIONS . . . . .	80
APPENDIX	
I. COMPUTER PROGRAMS . . . . .	82
II. TABLES OF COMPUTER RESULTS . . . . .	97
III. RENORMALIZED ENERGIES . . . . .	103
BIBLIOGRAPHY . . . . .	109

## LIST OF TABLES

Table		Page
1.	Curie Temperatures Given by Use of Two Different Terminations in Green Function Formalism Compared with High Temperature Expansion Results . . . . .	54
2.	Results for a F. C. C. Lattice with Spin $1/2$ for Termination Functions of the Type: $\alpha(x) = \langle S^z \rangle^x / 2S^{x+1}$ . . . . .	58
3.	Fraction of the Exchange Energy Present at the Curie Point . . . . .	70
4.	Computer Results for $\Phi_0$ and $\Phi_\delta$ for a Face-centered-cubic Lattice . . . . .	98
5.	Computer Results for $\Phi_0$ and $\Phi_\delta$ for a Body-centered-cubic Lattice . . . . .	99
6.	Computer Results for $\Phi_0$ and $\Phi_\delta$ for a Simple-cubic Lattice . . . . .	100
7.	Computer Results for Inverse Initial Susceptibility, $\mu H / 2SJM$ , for a Face-centered-cubic Lattice and the Function $\lambda(2\chi^{-1})$ . . . . .	101
8.	Computer Results for Inverse Initial Susceptibility, $\mu H / 2SJM$ , for a Body-centered-cubic Lattice and the Function $\lambda(2\chi^{-1})$ . . . . .	102

## LIST OF ILLUSTRATIONS

Figure		Page
1.	The Magnetization of EuO Compared with a Curve Calculated by the Green Function Technique . . . . .	53
2.	Theoretical Magnetization Curves in the Vicinity of the Curie Point for Four Values of Applied Field . .	56
3.	Magnetization as a Function of Applied Field, H, at the Curie Temperature . . . . .	57
4.	The Magnetization Curve for Nickel Compared with Three Theoretical Curves . . . . .	63
5.	Magnetization Curve for Iron Compared with Theoretical Curve . . . . .	64
6.	Derivative of the Square of the Relative Magnetization with Respect to the Relative Temperature from Nickel and from the Green Function Equations . . . . .	65
7.	Calculated Inverse Susceptibilities for a Face- centered-cubic Lattice with Spin Equal to $1/2$ . . . . .	66
8.	The Inverse Susceptibility versus Temperature Showing Asymptotic Convergence to the Weiss Molecular Field Result . . . . .	67
9.	The Relative Magnetic Energy of a Face-centered- cubic Lattice with $S = 1/2$ . . . . .	69
10.	The Specific Heat of a Face-centered-cubic Lattice with $S = 1/2$ . . . . .	71
11.	The Entropy of a Face-centered-cubic Lattice with $S = 1/2$ . . . . .	72

Figure		Page
12.	The Renormalization Factor for a Face-centered-cubic Lattice Plotted versus the Relative Temperature to the First Power and to the 5/2 Power . . . . .	74
13.	The Renormalization Factor for a Body-centered-cubic Lattice Plotted versus the Relative Temperature to the First Power and to the 5/2 Power . . . . .	75
14.	The Spin-spin Correlation Function $\langle S_o^- S_j^+ \rangle$ on a Logarithmic Scale versus the Relative Temperature . .	76
15.	The Spin-spin Correlation Function $\langle S_o^- S_j^+ \rangle$ versus the Distance along the (1 0 0) Direction . . . . .	77



## CHAPTER I

### INTRODUCTION

#### Weiss Molecular Field

The first good phenomenological theory of ferromagnetism was proposed by Pierre Weiss in 1907.<sup>1</sup> His theory was that each atom in a ferromagnetic substance was acted on not only by external magnetic induction fields but also by an internal field, the Weiss Molecular Field, which was in the same direction and linearly proportional to the average magnetization. The effective field that each atomic magnetic dipole moment sees according to this theory is  $\vec{H} + q\vec{M}$  where  $H$  is the applied field,  $M$  is the magnetization, and  $q$  is a constant on the order of  $10^7$  oe for iron and nickel. This theory gave results that were qualitatively right for the behavior of the magnetization and susceptibility. The Weiss model was quantitatively wrong at low temperatures in that it predicted a smaller decrease in  $M$  at low temperatures than was observed. For example, at a temperature 20% of the Curie temperature (the temperature where the spontaneous magnetization disappears) the decrease in the relative magnetization is predicted by the Weiss model to be 0.0002 as compared to the observed value for iron of about 0.01. Also above the Curie temperature,  $T_c$ , the Weiss model predicted that the inverse

susceptibility,  $\chi^{-1}$ , would vary like  $(T - T_c)$  which is observed for temperatures  $T$  much greater than  $T_c$ ; however, near  $T_c$ ,  $\chi^{-1}$  is observed to vary like  $(T - T_c)^{4/3}$ .<sup>9, 11, 12, 31</sup>

### The Heisenberg Ferromagnet

The origin of the strong interatomic coupling that must exist in ferromagnetic materials such as iron and nickel was not understood until 1928, when Heisenberg gave the first explanation based on quantum mechanics.<sup>2, 3</sup> Heisenberg's theory is that the coupling is due to the electrostatic interaction between electrons of different atoms whose wave functions overlap in space. In particular the coupling is due to the exchange term in the energy expression which is necessitated by the symmetry requirements on the wavefunction of two fermions and for this reason the interaction is called the "exchange interaction." Dirac<sup>4</sup> showed that except for a constant term which is not important the coupling between two electrons on atoms  $i$  and  $j$  was equivalent to a potential of the form:

$$V_{ij} = -2 J_{ij} \vec{S}_i \cdot \vec{S}_j \quad (1)$$

where  $\vec{S}_i$  is the spin angular momentum vector (operator) of atom  $i$  measured in units of  $\hbar$  and  $J_{ij}$  is the exchange integral of atoms  $i$  and  $j$ .

For the case in which this thesis is interested where there are a large number of atoms arranged on a crystal lattice, Equation (1) is generalized into the "Heisenberg Hamiltonian" operator for the whole system which is of the form:

$$\mathcal{H} = - \sum_i \sum_j J_{ij} \vec{S}_i \cdot \vec{S}_j - 2\mu H \sum_i S_i^z \quad (2)$$

where the sums over  $i$  and  $j$  range over all of the atoms in the system. The second term on the right is interaction of an external field,  $H$ , with the magnetic moment,  $\mu$ , associated with each unit of spin ( $\hbar/2$ ). The "z" direction is defined by  $\vec{H}$  and  $S_i^z$  is the "z" component of the  $\vec{S}_i$  operator. It should be noted that the Heisenberg theory not only explains the origin of the "Molecular Field" but changes the mathematical form of the interaction.

The Heisenberg model is based on a solid where the magnetic electrons are in states localized about the lattice sites with exchange of electrons taking place between nearest neighbor pairs. The model does not take into account the spreading of the electronic energy levels into bands by the kinetic energy. While it is generally thought that this model may be very good for nonconducting ferromagnets such as EuO, its applicability to conductors such as iron and nickel is not certain. However,

the Heisenberg model seems to give better predictions for the magnetization of nickel at low temperatures than calculations that begin with an itinerant electron picture.<sup>38</sup>

From the comparisons of the results of the calculations done in this thesis and the experimental results for nickel and iron it appears that the Heisenberg model is very good for equilibrium properties if one adds a temperature dependent magnetic moment quenching factor. This factor seems to change in nickel from 0.606 at 0°K to 0.642 at 627°K. This might be explained as a change in the magnetic polarization of the 4s conduction band which is partially polarized antiparallel to the more localized 3d electrons.

In some ways the Heisenberg Hamiltonian is very simple. The physical model that is used with it consists of a large number,  $N$ , of spins on a typical lattice. The system can be completely described in the quantum mechanical sense by describing the spin state of each lattice site; that is, no knowledge of the real-space wave functions is necessary other than the constant values of the integrals  $J_{ij}$  which for the cases considered in this paper are assumed to be zero unless  $i$  and  $j$  are nearest neighbors where  $J_{ij} = J$ . This is because once the spin state is known, the Fermi statistics fix the real space wave functions. Also the system has a well defined ground state with all spins aligned in the  $z$  direction. The excited states with one reversed spin are given by

$$| \vec{k} \rangle = N^{-1/2} \sum_j e^{i\vec{j} \cdot \vec{k}} S_j^- | 0 \rangle = S_{\vec{k}}^- | 0 \rangle \quad (3)$$

where  $| 0 \rangle$  is the ground state and  $S_j^-$  is the operator that reduces the z component of the spin at the j'th lattice site by one unit. The operator  $S_{\vec{k}}^-$  defined by Eq. (3) is the spinwave creation operator. The vector  $\vec{k}$  may be any of the vectors in the lattice's reciprocal space which is defined as the set of vectors  $\vec{k}$  such that for  $i = x, y, \text{ or } z$ ,  $k_i = 2\pi n_i / L_i$  where  $n_i$  is an integer and  $L_i$  is the length of the lattice in the  $i$  direction in lattice units. For a simple-cubic lattice containing  $N$  lattice points in real space this set can be reduced to a complete set of  $N$  nonequivalent vectors.<sup>5</sup> One such set can be constructed by requiring

$(0 \leq n_x < L_x, 0 \leq n_y < L_y, 0 \leq n_z < L_z)$ . The addition of another atom to the cubic unit cell to make a body-centered-cubic lattice requires that another set of  $N$  points be added to  $\vec{k}$  space to have a complete set. This additional set of points can be constructed by either letting

$$(L_x \leq n_x < 2L_x, 0 \leq n_y < L_y, 0 \leq n_z < L_z) \text{ or } (0 \leq n_x < L_x, L_y \leq n_y < 2L_y,$$

$0 \leq n_z < L_z) \text{ or } (0 \leq n_x < L_x, 0 \leq n_y < L_y, L_z \leq n_z < 2L_z)$ . All three sets of points defined in the last sentence must be added to the simple cubic set for a body-centered-cubic lattice. These sets are complete in the sense that

$$N^{-1} \sum_{\mathbf{k}} e^{i\vec{\mathbf{k}} \cdot \vec{\mathbf{j}}} = \delta_{\mathbf{j}} \quad (3a)$$

$$N^{-1} \sum_{\mathbf{j}} e^{i\vec{\mathbf{k}} \cdot \vec{\mathbf{j}}} = \delta_{\mathbf{k}}$$

where  $\delta_{\mathbf{j}}$  is the Kronecker delta function.

The energy of the state defined by Eq. (3) is given by

$$\mathcal{K} | \mathbf{k} \rangle = 2SJ(\gamma_0 - \gamma_{\mathbf{k}}) | \mathbf{k} \rangle \quad (3b)$$

$$= E_{\mathbf{k}}^{\text{sw}} | \mathbf{k} \rangle$$

where

$$\gamma_{\mathbf{k}} = \sum_{\delta} e^{i\vec{\mathbf{k}} \cdot \vec{\delta}} \quad (3c)$$

and  $\delta$  represents the set of vectors in real space that join a lattice site to its nearest neighbors.

Spinwave theory uses as a basis the set of states created by acting on the ground state with all possible combinations and numbers of the  $N$  spinwave creation operators. To see why this leads to difficulties at higher temperatures, consider the set of spinwave states with two reversed spins.

$$|k_1, k_2\rangle = S_{k_1}^- S_{k_2}^- |0\rangle \quad (3d)$$

Acting on this state with the Hamiltonian produces

$$\mathcal{H} |k_1, k_2\rangle = (E_{k_1}^{sw} + E_{k_2}^{sw}) |k_1 k_2\rangle \quad (3e)$$

$$- 2JN^{-1} \sum_k (\gamma_{k_1-k} - \gamma_k) |k, k_1 + k_2 - k\rangle$$

which shows that the two spinwave state is not exactly an eigenstate of the Hamiltonian. Usually the non-diagonal term is treated as an interaction term and perturbation theory is used to find renormalized energies which are temperature dependent due to the interaction between a spinwave and other thermally excited spinwaves. If the diagonal part of the last equation (i.e.  $k = k_1$  or  $k = k_2$ ) is used as the interaction energy between  $k_1$  and  $k_2$ , the renormalized energy for  $k$  would be

$$\begin{aligned} E_{k_1}^{sw}(T) &= E_{k_1}^{sw} - 2JN^{-1} \sum_{k_2} n_{k_2} (\gamma_0 - \gamma_{k_2} + \gamma_{k_1-k_2} - \gamma_{k_1}) \quad (3f) \\ &= J \left[ 1 - 2N^{-1} \sum_{k_2} n_{k_2} (\gamma_0 - \gamma_{k_2}) / \gamma_0 \right] (\gamma_0 - \gamma_{k_1}) \end{aligned}$$

$$n_{k_2} = 1 / \left( \exp(E_{k_2}^{sw}(T)/k_B T) - 1 \right) \quad (3g)$$

The renormalized energies,  $E_k^{sw}(T)$ , derived in this way agree with those M. Bloch found by minimizing the free energy<sup>36</sup> and those Dyson found by considering the Born scattering of two spinwaves.<sup>7</sup> The temperature dependence is contained in the term in square brackets which Dyson showed varied at low temperatures like  $1 - c_2(T/T_c)^{5/2}$  which is a slower decrease than  $\langle S^z \rangle$  which decreases like  $1 - c_1(T/T_c)^{3/2}$ . The constants  $c_1$  and  $c_2$  are of the same order of magnitude. A more detailed discussion of the renormalized spinwave is contained in Appendix III.

The difficulty of using the spinwave states as basis for any type of perturbation theory is due to the fact that for more than one reversed spin they are not an orthogonal set and therefore are not the eigenstates of any Hermitian operator. Consider the Hilbert space of states with  $n$  reversed spins on a lattice of  $N$  spins with  $S = 1/2$ . An orthogonal basis for this space is the set of states built up by acting on the ground state with all possible products of  $n$  operators that reverse the spin on a particular site,  $S_j^-$ . Since the  $S_j^-$  operators commute for different values of  $j$ , and for  $S = 1/2$  none of the  $n$  values of  $j$  can be the same; the number of distinct states,  $D_{n,N}$  is given by



$$D_{n,N} = \frac{N!}{n!(N-n)!}$$

The value of  $D_{n,N}$  is also the dimension of the space. Since the space is preserved under the Hamiltonian, it contains  $D_{n,N}$  eigenstates. The spinwave picture represents this space by the set of states produced by acting on the ground state with all possible products of  $n$  spinwave operators,  $S_k^-$ . The  $S_k^-$  operators commute for different values of  $k$ , but there is no rule limiting the number of times a single value of  $k$  can be repeated. The number of spinwave states in the space is

$$B_{n,N} = \frac{(N+n-1)!}{n!(N-1)!}$$

which exceeds the dimensionality of the space. Dyson shows that the effect of this surplus of states is to add a term to the free energy proportional to  $\exp(J/k_B T)$ . He argues that since this term decreases as  $T$  goes to zero faster than any positive power of  $T$ , it will not affect the power series in  $T$  of the free energy but will only limit the range of validity. He estimates that this range is up to a value of  $T$  such that the magnetization has decreased to about 75% of its value at zero temperature.<sup>7</sup>

There are also methods of finding the properties of the Heisenberg ferromagnet at temperatures above the Curie point. The first of these was developed by Peter Weiss from a technique used by Bethe and Peierls in

the order-disorder problem. Known as the BPW theory, it treats the interaction between a given atom and its nearest neighbors exactly but averages over the effect of the rest of the lattice on this unit.<sup>2, 8</sup>

Opechowski introduced a method of expanding the partition function of a Heisenberg ferromagnet in powers of  $(1/T)$ .<sup>10</sup> Domb and Sykes have used this technique to show theoretically the  $\chi^{-1} = A(T - T_c)^{4/3}$  behavior for  $T$  slightly greater than  $T_c$  of the Heisenberg ferromagnet which is similar to the behavior observed for nickel and iron.<sup>9, 11, 12</sup>

### Temperature Dependent Green Functions

The fault of the techniques described in the preceding section for the Heisenberg model is that there is a range of temperatures in the vicinity of the Curie temperature where neither technique is valid. The convergence of the  $(1/T)$  series becomes slow as  $T \rightarrow T_c^+$  and the spinwave interactions become large for  $T > 0.5 T_c$ . The application of a temperature-dependent, double-time Green function formalism to the Heisenberg ferromagnet problem by Bogolyubov and Tyablikov offered a means of finding solutions over the entire range.<sup>13, 14, 15</sup>

The problem with the Green function technique is that the equations are not in closed form. The time derivative of the first order Green function has a term which is proportional to higher order Green functions, and there is a similar relation between each Green function and the higher order Green functions. In order to find approximate

solutions it is necessary to break up this hierarchy of equations. Some work has been done by decoupling in the second order equation and good results for life times of spinwaves and bound-spin states at low temperatures have been obtained; however, the resulting equations are not presently solvable over the whole temperature range even using a computer.<sup>16,17,18</sup> In this paper, as in some previous works, the decoupling has been done in the first order equation by approximating the second order Green function as a function of first order Green functions.<sup>14,19</sup>

•

The decoupling used here was chosen because it seems to be required by certain theoretical and phenomenological criteria.

## CHAPTER II

### REVIEW OF GREEN FUNCTION THEORY

#### Properties of Green Functions

The following review of the properties of the temperature-dependent, double-time Green functions is patterned after the more general presentation in a review paper by Zubarev.<sup>15</sup> The retarded and advanced Green functions for a pair of Heisenberg operators  $A(t)$ ,  $B(t)$  is defined as follows

$$G_r(t) = -i \theta(t) \langle [A(t), B(0)] \rangle \quad (4)$$

$$G_a(t) = i \theta(-t) \langle [A(t), B(0)] \rangle$$

$$\theta(t) = 1 \quad \text{if } t > 0$$

$$0 \quad \text{if } t < 0$$

where the square brackets indicate the commutator and the angular brackets indicate an average over the canonical ensemble:

$$\langle A(t) \rangle = Q^{-1} \left\{ \exp(-\beta \mathcal{K}) A(t) \right\} \quad (5)$$

$$Q = \text{Tr} \left\{ \exp(-\beta \mathcal{K}) \right\}$$

The symbol  $\beta$  represents the inverse of the product of Boltzmann's constant and the absolute temperature,  $Q$  is the partition function, and  $\text{Tr}$  indicates the sum of the diagonal matrix elements of the operator it precedes.

The following time correlation functions will be necessary.

$$F_{AB}(t) = \langle A(t) B(0) \rangle \quad (6)$$

$$F_{BA}(t) = \langle B(0) A(t) \rangle$$

The time correlation functions do not contain the step function  $\theta(t)$  and are defined for  $t = 0$  where they give the expectation value for products of operators,  $F_{AB}(0) = \langle AB \rangle$ .

The spectral representation of the time correlation functions is obtained by considering the eigenfunctions  $|C_v\rangle$  and eigenvalues  $E_v$  of the Hamiltonian  $\mathcal{K}$ .

$$\mathcal{K} |C_v\rangle = E_v |C_v\rangle \quad (7)$$

By using the definition of averaging over the canonical ensemble,

$\langle \rangle$ ,  $F_{BA}(t)$  can be written:

$$\langle B(o) A(t) \rangle = Q^{-1} \sum_{\mathbf{v}} \langle C_{\mathbf{v}} | B(o) A(t) | C_{\mathbf{v}} \rangle \exp(-\beta E_{\mathbf{v}}) \quad (8)$$

where

$$Q = \sum_{\mathbf{v}} \exp(-\beta E_{\mathbf{v}})$$

By the completeness property of the set  $| C_{\mathbf{v}} \rangle$  and the definition of  $A(t)$  in units such that  $\hbar = 1$ ,

$$A(t) = \exp(-i\mathcal{H}t) A(o) \exp(i\mathcal{H}t) \quad (9)$$

Eq. (8) can be written

$$\langle B(o) A(t) \rangle = Q^{-1} \sum_{\mathbf{v}} \sum_{\mathbf{u}} \langle C_{\mathbf{v}} | B(o) | C_{\mathbf{u}} \rangle \langle C_{\mathbf{u}} | A(o) | C_{\mathbf{v}} \rangle \quad (10)$$

$$\times \exp(-\beta E_{\mathbf{v}} - i(E_{\mathbf{v}} - E_{\mathbf{u}}) t)$$

also

$$\langle A(t) B(o) \rangle = Q^{-1} \sum_{\mathbf{v}} \sum_{\mathbf{u}} \langle C_{\mathbf{v}} | A(o) | C_{\mathbf{u}} \rangle \langle C_{\mathbf{u}} | B(o) | C_{\mathbf{v}} \rangle \quad (11)$$

$$\times \exp(-\beta E_{\mathbf{v}} + i(E_{\mathbf{v}} - E_{\mathbf{u}}) t)$$

By interchanging u and v in Eq. (11), Eq. (10) and (11) can be written

$$F_{BA}(t) = \int_{-\infty}^{\infty} J(\omega) \exp(-i\omega t) d\omega \quad (12)$$

$$F_{AB}(t) = \int_{-\infty}^{\infty} J(\omega) \exp(i\omega t) \exp(\beta\omega) d\omega$$

where

$$J(\omega) = \quad (13)$$

$$Q^{-1} \sum_u \sum_v \langle C_v | A(o) | C_u \rangle \langle C_u | B(o) | C_v \rangle \exp(-\beta E_u) \delta(E_u - E_v - \omega)$$

The function  $J(\omega)$  is the spectral intensity of  $F_{BA}(t)$ .

The spectral representations of the advanced and retarded Green functions are obtained from the spectral representations of the time correlation functions. The Fourier component of  $G_r(t)$ ,  $G_r^i(E)$ , is defined as

$$G_r(t) = \int_{-\infty}^{\infty} G_r^i(E) \exp(-iEt) dt \quad (14)$$

$$G_r^i(E) = \frac{1}{2\pi} \int_{-\infty}^{\infty} G_r(t) \exp(iEt) dE \quad (15)$$

By using the definition of  $G_r(t)$ , Eq. (4), and Eq. (12),  $G_r'(E)$  can be written in terms of  $J(\omega)$

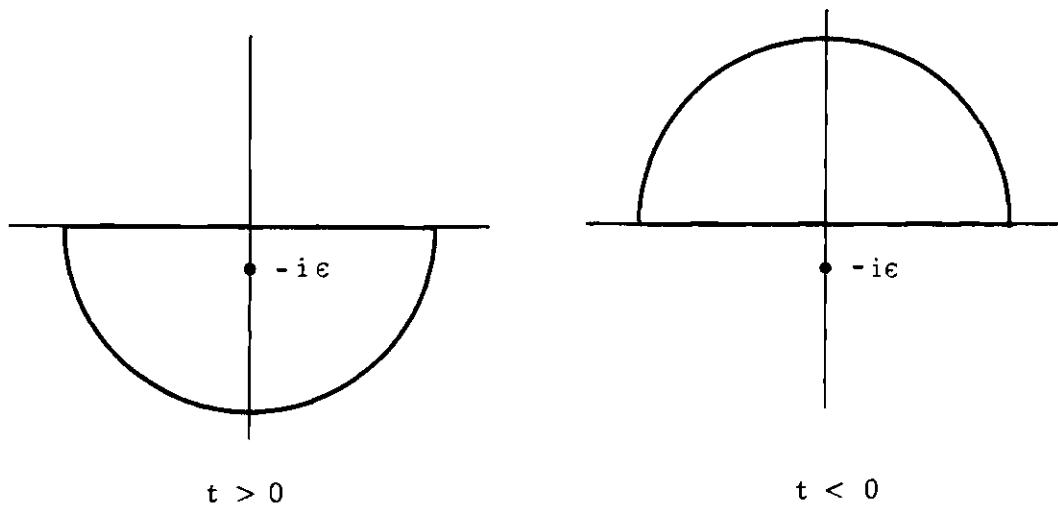
$$G_r'(E) = \frac{1}{2\pi i} \int_{-\infty}^{\infty} \exp(iEt) \theta(t) (F_{AB} - F_{BA}) dt \quad (16)$$

$$= \int_{-\infty}^{\infty} J(\omega) (\exp(\beta \omega) - 1) \frac{1}{2\pi i} \int_{-\infty}^{\infty} \exp(i(E-\omega)t) \theta(t) dt d\omega$$

The step function  $\theta(t)$  can be written in the form

$$\theta(t) = \lim_{\epsilon \rightarrow 0^+} \frac{1}{2\pi} \int_{-\infty}^{\infty} \frac{\exp(-ixt)}{x + i\epsilon} dx \quad (17)$$

To verify Eq. (17), consider  $x$  as the real part of a complex variable and that the integral is taken over one of the contours shown below.





The integrand has a pole in the lower half plane at  $x = -i\epsilon$ . When  $t > 0$  the contour must be closed in the lower half plane and the right side of Eq. (17) is equal to one by Cauchy's Integral Law. If  $t < 0$  then the contour must be closed in the upper half plane and does not enclose the pole, so the right side of Eq. (17) is zero. Since these are the defining properties of  $\theta(t)$ , as given by Eq. (4), Eq. (17) is valid.

Now one factor in the right side of Eq. (16) can be written

$$\begin{aligned} \int_{-\infty}^{\infty} \exp(i(E-\omega)t) \theta(t) dt &= \frac{1}{2\pi} \int_{-\infty}^{\infty} \int_{-\infty}^{\infty} \frac{\exp(i(E-\omega-x)t)}{x+i\epsilon} dx dt \\ &= \frac{1}{E-\omega+i\epsilon} \end{aligned} \quad (18)$$

Since

$$\frac{1}{2\pi} \int_{-\infty}^{\infty} \exp(i(E-\omega-x)t) dt = \delta(E-\omega-x) \quad (19)$$

Thus the Fourier component of  $G_r(t)$ , Eq. (16) is given by

$$G'_r(E) = \lim_{\epsilon \rightarrow 0^+} \frac{1}{2\pi} \int_{-\infty}^{\infty} \frac{(\exp(\beta\omega) - 1) J(\omega) d\omega}{E - \omega + i\epsilon} \quad (20)$$

A similar calculation for the advanced Green function yields

$$G_a'(E) = \lim_{\epsilon \rightarrow 0^+} \frac{1}{2\pi} \int_{-\infty}^{\infty} \frac{(\exp(\beta \omega) - 1) J(\omega) d\omega}{E - \omega - i\epsilon} \quad (21)$$

An important property of  $G_r'(E)$  is that it can be continued analytically into the upper complex plane for  $E = \alpha + i\lambda$  where  $\lambda > 0$ . When  $\lambda > 0$  the limit  $\epsilon \rightarrow 0^+$  can be taken by setting  $\epsilon = 0$ . Similarly  $G_a'(E)$  can be continued analytically into the lower complex plane ( $\lambda < 0$ ). In this case

$$G_r'(E) = \lim_{\epsilon \rightarrow 0^+} G_r'(E + i\epsilon) \quad (E \text{ real}) \quad (22)$$

$$G_a'(E) = \lim_{\epsilon \rightarrow 0^+} G_a'(E - i\epsilon)$$

Taking the difference between Eq. (20) and (21) and using Eq. (22)

$$\lim_{\epsilon \rightarrow 0^+} (G_r'(E + i\epsilon) - G_a'(E - i\epsilon)) \quad (23)$$

$$\begin{aligned} &= \lim_{\epsilon \rightarrow 0^+} \frac{1}{2\pi} \int_{-\infty}^{\infty} (\exp(\beta \omega) - 1) J(\omega) \left[ \frac{1}{E - \omega + i\epsilon} - \frac{1}{E - \omega - i\epsilon} \right] d\omega \\ &= -i(\exp(\beta E) - 1) J(E) \end{aligned}$$

where  $E$  is real since

$$\lim_{\epsilon \rightarrow 0} \frac{1}{E - \omega + i\epsilon} - \frac{1}{E - \omega - i\epsilon} = -2\pi i \delta(E - \omega) \quad (24)$$

Equations (22) and (12) can be used to write the time dependent correlation functions in terms of the Green function.

$$F_{AB}(t) = A(t) B(0) \quad (25)$$

$$= \lim_{\epsilon \rightarrow 0^+} -i \int_{-\infty}^{\infty} \frac{\exp(-i\omega t)}{\exp(-\beta\omega) - 1} \left( G_r'(\omega + i\epsilon) - G_a'(\omega - i\epsilon) \right) d\omega$$

Therefore if solutions for the Green functions can be found, so can those physical properties which are determined by the time correlation function.

### Green Function for the Heisenberg Magnet

For the case where only the nearest neighbor interaction is of importance, the Heisenberg Hamiltonian, Eq. (2) can be written as

$$\mathcal{H} = J \sum_j \sum_{\delta} \left( S_j^z S_{j+\delta}^z + S_j^x S_{j+\delta}^x + S_j^y S_{j+\delta}^y \right) - 2\mu H \sum_j S_j^z \quad (26)$$

where  $j$  is summed over the lattice and  $\delta$  is summed over the nearest neighbor vectors.

Since the raising and lowering operators are defined by

$$S_j^+ = S_j^x + iS_j^y \quad (27)$$

$$S_j^- = S_j^x - iS_j^y$$

and have the commutation rules

$$[S_j^+, S_i^-] = 2S_k^z \delta_{j,i} \quad (28)$$

$$[S_j^+, S_i^z] = S_j^+ \delta_{j,i}$$

Equation (26) can be written

$$\mathcal{H} = -J \sum_j \sum_{\delta} (S_j^z S_{j+\delta}^z + S_j^+ S_{j+\delta}^-) - 2\mu H \sum_j S_j^z \quad (29)$$

The particular first order, or one particle, Green function used is defined as

$$G(j, t) = -i \theta(t) \langle [S_j^-(t), S_o^+(o)] \rangle \quad (30)$$

$$\theta(t) = 1 \text{ if } t > 0$$

$$0 \text{ if } t < 0$$

The equation of motion of  $G(j, t)$  is

$$\begin{aligned}
 i \frac{d}{dt} G(j, t) = & \delta(t) \langle [S_j^-(t), S_o^+(o)] \rangle \\
 & + \theta(t) \langle \left[ \frac{d}{dt} S_j^-(t), S_o^+(o) \right] \rangle
 \end{aligned} \tag{31}$$

The time derivative of the operator is given by (for  $\hbar = 1$ )

$$i \frac{d}{dt} S_j^-(t) = [S_j^-(t), \mathcal{H}] \tag{32}$$

Using Equations (20), (28), and (29), Eq.(31) becomes

$$\begin{aligned}
 i \frac{d}{dt} G(j, t) = & 2\delta(t) \delta_j \langle S_j^z \rangle + 2\mu H G(j, t) \\
 & + 2Ji\theta(t) \sum_{\delta} \langle [S_{j+\delta}^z(t) S_j^-(t), S_o^+(o)] \rangle \\
 & - 2Ji\theta(t) \sum_{\delta} \langle [S_j^z(t) S_{j+\delta}^-(t), S_o^+(o)] \rangle
 \end{aligned} \tag{33}$$

where  $\delta(t)$  is the Dirac delta function and  $\delta_j$  is the Kronecker delta,  $\delta_{j,o}$ . The right side of Eq. (33) contains two terms which involve higher order Green functions when the  $S_j^z$  operator in the commutator is expanded in terms of  $S_j^+$  and  $S_j^-$  operators. For example

$$S_j^z = S - S_j^- S_j^+ \quad (\text{for } S = 1/2) \quad (34)$$

The method of decoupling used here was originated by Callen,<sup>19</sup> and is most easily described for the case  $S = 1/2$ . In addition to Eq. (34),  $S_j^z$  can also be written

$$S_j^z = 1/2(S_j^+ S_j^- - S_j^- S_j^+) \quad (35)$$

by rewriting Eq. (28). By multiplying Eq. (34) by an arbitrary parameter  $\alpha$  and Eq. (35) by  $(1 - \alpha)$  and adding it follows that:

$$S_j^z = \alpha S + (1/2)(1 - \alpha)S_j^+ S_j^- - (1/2)(1 + \alpha)S_j^- S_j^+ \quad (36)$$

Using Eq. (36) in the second term on the right side of Eq. (33) produces:

$$\langle [S_{j+\delta}^z(t) S_j^-(t), S_o^+(o)] \rangle = \alpha S \langle [S_j^-(t), S_o^+(t)] \rangle \quad (37)$$

$$+ (1/2)(1 - \alpha) \langle [S_{j+\delta}^+(t) S_{j+\delta}^-(t) S_j^-(t), S_o^+(o)] \rangle$$

$$- (1/2)(1 - \alpha) \langle [S_{j+\delta}^-(t) S_{j+\delta}^+(t) S_j^-(t), S_o^+(o)] \rangle$$

The higher order Green functions are decoupled in the following symmetric way:

$$\begin{aligned} \langle [S_{j+\delta}^+(t) S_{j+\delta}^-(t) S_j^-(t), S_o^+(o)] \rangle \rightarrow \langle S_{j+\delta}^+(t) S_{j+\delta}^-(t) \rangle \langle [S_j^-(t), S_o^+(o)] \rangle \\ + \langle S_j^-(t) S_{j+\delta}^+(t) \rangle \langle [S_{j+\delta}^-(t), S_o^+(o)] \rangle \end{aligned} \quad (38)$$

This is analogous to the Hartree-Fock procedure in second quantization theory.<sup>20</sup> After decoupling Eq. (37) becomes;

$$\begin{aligned} \langle [S_{j+\delta}^z(t) S_j^-(t), S_o^+(o)] \rangle = \langle S_j^z \rangle \langle [S_j^-(t), S_o^+(o)] \rangle \\ - \alpha \langle S_j^- S_{j+\delta}^+ \rangle \langle [S_{j+\delta}^-(t), S_o^+(o)] \rangle \end{aligned} \quad (39)$$

When no times are shown for operators, all of the operators in the angular brackets are at the same time making the resulting expectation value independent of time. Also since  $\langle S_j^z \rangle$  is independent of  $j$ , it may be written simply  $\langle S^z \rangle$ . The third term on the right of Eq. (33) is identical to the second if the subscripts  $j$  and  $j + \delta$  are interchanged.

As Callen points out, if  $\alpha$  is set equal zero, the result will be the same as setting the operator  $S_j^z$  in Eq. (33) equal to the number

$\langle S^z \rangle$ . This is what Tyablikov did and obtained spinwave energies at low temperatures proportional to  $\langle S^z \rangle$  which would decrease like  $(1 - c_1 T^{3/2})$  in disagreement with spinwave theory's prediction of a  $(1 - c_2 T^{5/2})$  dependence.<sup>7, 14, 15, 19, 22</sup> His results over the higher temperature range are in agreement with the present results.

Callen reasoned that  $\alpha$  should be approximately equal to unity when  $\langle S^z \rangle = S$  because an approximation of  $S_j^z$  based on Eq. (32) would be more accurate in this region of temperature. Also he reasoned that  $\alpha$  should go to zero as  $\langle S^z \rangle \rightarrow 0$  since an approximation of  $S_j^z$  based on Eq. (35) should be more accurate. As shall be shown later, these same requirements are necessary in order that agreement with spinwave theory shall be obtained at low temperatures ( $\langle S^z \rangle = S$ ) and that a finite Curie temperature shall exist. The termination function,  $\alpha$ , chosen by Callen was  $\langle S^z \rangle / 2S^2$  for arbitrary  $S$ . Since the requirements above do not completely determine  $\alpha$ , the first step of this work was to find additional physical criteria that would more completely determine  $\alpha$ . This determination is covered by Chapter V. The resulting function is

$$\alpha = \langle S^z \rangle^3 / 2S^4 \quad (40)$$



There will be more discussion on this form later. For the rest of the development of the Green function equations  $\alpha$  will be left arbitrary. The equation of motion for  $G(j, t)$ , Eq.(33), can now be written as:

$$\left( i \frac{d}{dt} - 2\mu H + 2J \gamma_0 ( \langle S^z \rangle + \alpha \langle S_o^+ S_\delta^- \rangle ) \right) G_{(j, t)} \quad (41)$$

$$- 2J \sum_{\delta} \left( \langle S^z \rangle + \alpha \langle S_o^+ S_j^- \rangle \right) G(j + \delta, t) = 2\delta(t) \delta(j) \langle S^z \rangle$$

Looking back over Eq. (4) and (30) through (41) it can be seen that Eq. (41) would be equally valid if  $G(j, t)$  had been defined as the advanced Green function rather than the retarded Green function. By Eq. (25)

$$\langle S_j^-(t) S_o^+(0) \rangle = \lim_{\epsilon \rightarrow 0^+} -i \int_{-\infty}^{\infty} \frac{\exp(-i\omega t)}{\exp(-\omega/\beta) - 1} \left( G'(j, \omega + i\epsilon) - G'(j, \omega - i\epsilon) \right) d\omega$$

In order to find  $G'(j, \omega)$ ,  $G(j, t)$  in Eq. (41) is replaced by the expression on the right side of Eq. (14)

$$\int_{-\infty}^{\infty} \left\{ i \frac{d}{dt} - 2\mu H + 2J\gamma_0 ( \langle S^z \rangle + \alpha \langle S_o^+ S_{\delta}^- \rangle ) G'(j, E) \right. \quad (43)$$

$$\left. - 2J \sum_{\delta} ( \langle S^z \rangle + \alpha \langle S_o^+ S_{\delta}^- \rangle ) G'(j + \delta, E) \right\} \exp(-iEt) dE$$

$$= 2 \delta(t) \delta_j \langle S^z \rangle$$

By multiplying both sides of Eq. (43) by  $(1/2\pi) \exp(i\omega t)$  and integrating over  $t$  one obtains

$$\left( \omega - 2\mu H + 2J\gamma_0 ( \langle S^z \rangle + \alpha \langle S_o^+ S_{\delta}^- \rangle ) \right) G'(j, \omega) \quad (44)$$

$$- 2J \sum_{\delta} ( \langle S^z \rangle + \alpha \langle S_o^+ S_{\delta}^- \rangle ) G'(j + \delta, \omega) = \pi^{-1} \langle S^z \rangle \delta_j$$

Notice that  $\langle S_o^+ S_{\delta}^- \rangle$  is independent of the particular nearest neighbor vector  $\delta$  and can be moved out of the summation. At this point it is convenient to represent  $G'(j, \omega)$  as

$$G'(j, \omega) = \frac{1}{N} \sum_{\mathbf{k}'} G'(\mathbf{k}, \omega) \exp(i\vec{k}' \cdot \vec{j}) \quad (45)$$

where  $k$  ranges over the set of  $N$  vectors defined after Eq. (3). By using Eq. (45) within Eq. (44) and then multiplying by  $\exp(-ik \cdot j)$  and summing over  $j$ , Eq. (44) becomes

$$\begin{aligned} \left[ \omega - 2\mu H' + 2J(\langle S^z \rangle + \alpha \langle S_o^+ S_\delta^- \rangle)(\gamma_o - \gamma_k) \right] G'(k, \omega) \\ = \pi^{-1} \langle S^z \rangle \end{aligned} \quad (46)$$

The solution to this equation is

$$G'(k, \omega) = \frac{\pi^{-1} \langle S^z \rangle}{\omega + E_k} \quad (47)$$

where

$$E_k = -2\mu H' + 2J(\langle S^z \rangle + \alpha \langle S_o^+ S_\delta^- \rangle)(\gamma_o - \gamma_k) \quad (48)$$

It is now apparent that the temperature dependent renormalized energies,  $E_k$ , are dependent on the termination function,  $\alpha$ .

By using Eq. (47) and (45) in Eq. (42)

$$\langle S_j^-(t) S_o^+(o) \rangle = \quad (49)$$

$$\lim_{\epsilon \rightarrow 0^-} \sum_k \frac{i \langle S^z \rangle}{\pi N} \int_{-\infty}^{\infty} \frac{\exp(ik \cdot j - i\omega t)}{\exp(-\beta\omega) - 1} \left( \frac{1}{\omega + E_k + i\epsilon} - \frac{1}{\omega + E_k - i\epsilon} \right) d\omega$$

Again using Eq. (24)

$$\langle S_j^-(t) S_o^+(o) \rangle = \frac{2 \langle S^z \rangle}{N} \sum_k \frac{\exp(ik \cdot j - i\omega t)}{\exp(\beta E_k) - 1} \quad (50)$$

For the case  $S = 1/2$ , the relative magnetization is given by

$$M = 2 \langle S^z \rangle = 2S - 2 \langle S_o^- S_o^+ \rangle \quad (51)$$

Utilizing the expression for  $\langle S_o^- S_o^+ \rangle$  from Eq. (50)

$$M = 1 - \frac{4 \langle S^z \rangle}{N} \sum_k \frac{1}{\exp(\beta E_k) - 1} \quad (51a)$$

Eq. (51) may be written in the form

$$M = \frac{1}{1 + 2 \phi_o} \quad (51b)$$

where

$$\Phi_j = \frac{1}{N} \sum_k \frac{\exp(ik \cdot j)}{\exp(\beta E_k) - 1} \quad (51c)$$

The magnetic energy of the spin system can be evaluated by finding the expectation value of the Hamiltonian, Eq. (26).

$$\langle \mathcal{H} \rangle = - NJ \gamma_o \left( \langle S_o^z S_\delta^z \rangle + \langle S_o^+ S_\delta^- \rangle \right) + 2N\mu H \langle S^z \rangle \quad (52)$$

The correlations of the  $z$  components appearing in Eq. (52) may be written in the following form for  $S = 1/2$ .

$$\begin{aligned} \langle S_o^z S_\delta^z \rangle &= \langle (S - S_o^- S_o^+) (S - S_\delta^- S_\delta^+) \rangle \\ &= S^2 - 2\langle S_o^- S_o^+ \rangle + \langle S_o^- S_o^+ S_\delta^- S_\delta^+ \rangle \end{aligned} \quad (53)$$

In order to find the last term on the right of Eq. (53) exactly it is necessary to have a solution for the second order Green function involving four operators. In the spirit of this work it can be contracted by the same procedure that was used to contract the second order Green function.

$$\langle S_o^- S_o^+ S_\delta^- S_\delta^+ \rangle \rightarrow \langle S_o^- S_o^+ \rangle \langle S_\delta^- S_\delta^+ \rangle + \alpha \langle S_o^- S_\delta^+ \rangle \langle S_o^+ S_\delta^- \rangle \quad (55)$$

When this is done Eq. (52) and (53) become

$$\langle S_o^z S_\delta^z \rangle = \langle S^z \rangle^2 + \alpha \langle S_o^- S_\delta^+ \rangle^2 \quad (56)$$

$$\langle \mathcal{K} \rangle = - NJ_o \left( \langle S^z \rangle^2 + \langle S_o^- S_\delta^+ \rangle + \alpha \langle S_o^- S_\delta^+ \rangle^2 \right) \quad (57)$$

All of the expectation values on the right side of Eq. (57) can now be calculated by using Eq. (50), (47), and (40). Once  $\langle \mathcal{K} \rangle$  is known as a function of temperature the specific heat,  $d \langle \mathcal{K} \rangle / dT$ , and the entropy,  $dS = d \langle \mathcal{K} \rangle / T$ , can be obtained.

#### Extending the Results to $S > 1/2$

The following technique for calculating  $\langle S^z \rangle$  for  $S > 1/2$  is due to Callen.<sup>19</sup> He used the following Green function

$$G(a, j, t) = -i \theta(t) \langle [S_j^-(t), \exp(a S_o^z(o)) S_o^+(o)] \rangle \quad (58)$$

which reduces to the Green function defined in Eq. (30) when  $a = 0$ .

The equations of motion and termination procedure, Eq. (31) through

(44), are essentially the same for  $G(a, j, t)$  except for obvious substitutions. For example Eq. (44) will become

$$\left( \omega - 2\mu H + 2J\gamma_o \left( \langle S^z \rangle + \alpha \langle S_o^+ S_\delta^- \rangle \right) \right) G'(a, j, \omega) \quad (59)$$

$$- 2J \sum_{\delta} \left( \langle S^z \rangle + \alpha \langle S_o^+ S_\delta^- \rangle \right) G'(a, j, \omega)$$

$$= - \frac{1}{2\pi} \langle [S_j^-, \exp(-a S_o^z) S_o^+] \rangle$$

Equation (50) becomes

$$\langle S_j^-(t) \exp(a S_o^z(o)) S_o^+(o) \rangle \quad (60)$$

$$= - \frac{\langle [S_o^-, \exp(a S_o^z) S_o^+] \rangle}{N} \sum_k \frac{e^{ikj - i\omega t}}{\exp(\beta E_k) - 1}$$

where the  $E_k$  remain unchanged from Eq. (48). Callen's technique requires the following definitions

$$\beta(a) = \langle [S_o^- \exp(aS_o^z), S_o^+] \rangle \quad (61)$$

$$\Omega(a) = \langle \exp(aS_o^z) \rangle \quad (62)$$

$$\varphi(a) = \langle S_o^- \exp(aS_o^z) S_o^+ \rangle \quad (63)$$

$$D = \frac{d}{da} \quad (64)$$

Equation (60) implies

$$\varphi(a) = -\Phi_o \beta(a) \quad (65)$$

where  $\Phi_o$  was defined in Eq. (51c).

The following identity can be proved valid for all values of  $n$  by mathematical induction.

$$[S_o^+, (S_o^z)^n] = \{(S_o^z - 1)^n - (S_o^z)^n\} S_o^+ \quad (66)$$

This implies that

$$[S_o^+, \exp(aS_o^z)] = (e^{-a} - 1) \exp(aS_o^z) S_o^+ \quad (67)$$



and that

$$\begin{aligned}\beta(a) &= \langle S_o^- [\exp(aS_o^z), S_o^+] + [S_o^-, S_o^+] \exp(aS_o^z) \rangle \quad (68) \\ &= (1 - e^{-a}) \langle S_o^- \exp(aS_o^z) S_o^+ \rangle - 2 \langle S_o^z \exp(aS_o^z) \rangle\end{aligned}$$

Equation (67) can be written

$$\exp(aS_o^z) S_o^+ = e^a S_o^+ \exp(aS_o^z) \quad (69)$$

and used in Eq. (68) along with this identity from Pauli spin theory

$$S_o^- S_o^+ = S(S+1) - S_o^z - (S_o^z)^2 \quad (70)$$

These replacements put Eq. (68) in the form

$$\beta(a) = S(S+1) (e^a - 1) \langle \exp(aS_o^z) \rangle \quad (71)$$

$$- (e^a + 1) \langle S_o^z \exp(aS_o^z) \rangle - (e^a - 1) \langle (S_o^z)^2 \exp(aS_o^z) \rangle$$

$$\beta(a) = S(S+1) (e^a - 1) \Omega - (e^a + 1) D \Omega - (e^a - 1) D^2 \Omega \quad (72)$$

By using Eq. (69) and (70), Eq. (63) becomes

$$\varphi(a) = e^a \left[ S(S+1) \Omega - D \Omega - D^2 \Omega \right] \quad (73)$$

Now Eqs. (65), (72) and (73) can be used to find the differential equation for  $\Omega$  in terms of  $S$  and  $\Phi_0$ .

$$D^2 \Omega + \frac{(1 + \Phi_0) e^a + \Phi_0}{(1 + \Phi_0) e^a - \Phi_0} D \Omega - S(S+1) \Omega = 0 \quad (74)$$

The two boundary conditions required to solve Eq. (74) uniquely are given by Eq. (62)

$$\Omega(0) = 1 \quad (75)$$

and by the operator identity

$$\prod_{p = -S}^S (S^2 - p) = 0 \quad (76)$$

which by using Eq. (62) can be written

$$\prod_{p=-S}^S (D - p) \Omega(o) = 0 \quad (77)$$

The solution to Eq. (74) satisfying the boundary conditions, Eqs. (75) and (77), is

$$\Omega(a) = \frac{\phi_o^{2S+1} e^{-Sa} - (1 + \phi_o)^{2S+1} e^{(S+1)a}}{\left[ \phi_o^{2S+1} - (1 + \phi_o)^{2S+1} \right] \left[ (1 + \phi_o) e^a - \phi_o \right]} \quad (78)$$

The value of  $\langle S^z \rangle$  can be found by differentiation.

$$\langle S^z \rangle = D \Omega(o) = \frac{(S - \phi_o)(1 + \phi_o)^{2S+1} + (S + 1 + \phi_o) \phi_o^{2S+1}}{(1 + \phi_o)^{2S+1} - \phi_o^{2S+1}} \quad (79)$$

As expected Eq. (79) reduces to Eq. (50) for the case  $S = 1/2$ . This result also agrees with earlier work by Tahir-Kheli and ter Haar.<sup>22</sup>

## CHAPTER III

### CALCULATIONAL PROCEDURE

In order to calculate the physical properties of the Heisenberg ferromagnet by using the theoretical framework described in the last chapter, it is necessary to calculate the sums  $\Phi_0$  and  $\Phi_\delta$  defined by Eq. (51)

$$\Phi_j = \frac{1}{N} \sum_k^N \frac{\exp(ik \cdot j)}{\exp(E_k/k_B T) - 1} \quad (87)$$

where from Eq. (46)

$$E_k = 2\mu H' + JL(\gamma_0 - \gamma_k) \quad (88)$$

$$L = 2(\langle S^z \rangle + \alpha \langle S_0^+ S_\delta^- \rangle) \quad (89)$$

$$\gamma_k = \sum_{\delta} \exp(i\vec{k} \cdot \vec{\delta}) \quad (90)$$

where  $\delta$  as before signifies a nearest-neighbor vector or the set of nearest-neighbor vectors. These sums were calculated by using the

Algol program contained in Appendix I on a Burroughs' B-5500 computer. In Eq. (87) the simple cubic set of  $k$  vectors discussed in Chapter I is summed over. However for the body-centered-cubic and face-centered-cubic lattices, instead of adding additional sets of points to the summation it is easier to assign additional sets of energy values to the basic set of  $k$  vectors.<sup>22</sup> This procedure is equivalent to that used for the "optical modes" in lattice vibration theory. If the lattice consists of  $L_x$  by  $L_y$  by  $L_z$  lattice units ( $L_x L_y L_z = N/q$ ), then  $k = (k_x, k_y, k_z)$  where  $k_x = 2\pi n_x / L_x$ , etc., and  $n_x, n_y, n_z$  are integers,  $0 \leq n_x < L_x$ , etc. For the simple cubic lattice where the number of atoms per unit cell,  $q$ , is one, there is only one "mode of oscillation" and

$$\gamma_0 - \gamma_k = 6 - 2 \cos(k_x) - 2 \cos(k_y) - 2 \cos(k_z) \quad (\text{sc}) \quad (91)$$

For body-centered-cubic where  $q = 2$  and face-centered-cubic where  $q = 4$ , there will be  $q$  "modes of oscillation" indicated by the multiple signs in the following equations. For body-centered-cubic

$$\gamma_0 - \gamma_k = 8^{\pm} 8 \cos(k_x/2) \cos(k_y/2) \cos(k_z/2) \quad (\text{bcc}) \quad (92)$$

and for face-centered cubic

$$\gamma_0 - \gamma_k = \frac{12}{\pi} \left[ 4 \cos(k_x/2) \cos(k_y/2) \right] \quad (\text{fcc}) \quad (93)$$

$$\left[ 4 \cos(k_y/2) \cos(k_z/2) \right]$$

$$\left[ 4 \cos(k_z/2) \cos(k_x/2) \right]$$

Each mode is summed over  $k$ .

The problem is to find self consistent solutions to Eq. (87) for  $j = 0, \delta$  and to Eq. (88), since  $L$  is a function of  $\phi_\delta$  by Eqs. (40), (48), (79), and (89). The following technique is used to find solutions for zero applied field without reiteration. Define

$$R = k_B T / JL = \theta / L \quad (94)$$

where  $\theta$  is the temperature multiplied by Boltzmann's constant and divided by the exchange constant.

Equation (87) can be written in terms of  $R$

$$\phi_j = \frac{1}{N} \sum_k^N \frac{\exp(ik \cdot j)}{\exp((\gamma_0 - \gamma_k)/R) - 1} \quad (95)$$

The computer is now used to find  $\Phi_0$  and  $\Phi_\delta$  for a fixed value of  $R$ . Next  $L(\Phi_0, \Phi_\delta, S)$  is found from Eqs. (40), (48), and (79). The requirement for self consistency is satisfied if finally the reduced temperature,  $\theta$ , is set equal to  $LR$ , where  $R$  is the value initially chosen. As the parameter  $R$  is stepped from 0 to  $\infty$  by the computer, values of all the terms of interest are obtained for a set of values of  $\theta$  from zero to the Curie point,  $\theta_c$ , where  $\langle S^z \rangle$ ,  $L$ , and all  $E_k$  go to zero.

Results for  $\theta > \theta_c$  can be obtained if  $2\mu H'$  is set equal to a non zero value and the limit taken as  $2\mu H' \rightarrow 0$ . Experience with these calculations has shown that if  $\theta$  is more than 2% greater than  $\theta_c$ , the results for susceptibility, specific heat, and energy of nickel obtained for a value of  $2\mu H'$  equivalent to an applied field of 125 oe are essentially the same as the results for  $2\mu H' \rightarrow 0$  (see Fig. 7). The physical properties of interest in this region are the initial susceptibility,  $\chi = \lim(H \rightarrow 0) M/H$ , the specific heat which is proportional to  $\langle S_o^+ S_\delta^- \rangle$  in this region (Eqs. (52) and (57)), and the correlation function  $\langle S_o^+ S_j^- \rangle$  which is related to neutron magnetic scattering.

From Eq. (79) it can be seen that as  $\langle S^z \rangle \rightarrow 0$ ,  $\Phi_0 \rightarrow \infty$  and that in this limit

$$\langle S^z \rangle = \left( S(S+1)/3 \right) \Phi_0^{-1} \quad (96)$$

and from Eq. (48)

$$\langle S_o^+ S_j^- \rangle = \left( 2S(S+1)/3 \right) \Phi_j / \Phi_o \quad (97)$$

While  $\Phi_o$  and  $\Phi_j$  both become infinitely large as  $2\mu H' \rightarrow 0$  and  $\theta > \theta_c$ , their ratio is well behaved (see Chap. IV).

The specific heat,  $C$ , and the entropy,  $S$ , are calculated by starting the program with a small value of  $R$  and then increasing  $R$  by small increments so that each value of  $\theta$  calculated is only slightly larger than the preceding value. The value of  $\langle H \rangle$  is also calculated by using Eq. (52) and Eq. (57) for each  $\theta$ . If the set of  $\theta$ 's calculated are designated by  $\theta_n$  ( $\theta_n > \theta_{n-1}$ ) and the corresponding value of  $\langle H \rangle$  by  $E_n$ , and if  $\eta$  is the number of atoms per unit volume or per unit weight

$$C \left( (\theta_n + \theta_{n-1})/2 \right) \doteq -(\eta k_B/J)(E_n - E_{n-1})/(\theta_n - \theta_{n-1}) \quad (98)$$

$$S \left( (\theta_n + \theta_{n-1})/2 \right) \doteq - \sum_{n'=1}^n 2(\eta k_B/J)(E_{n'} - E_{n'-1})/(\theta_{n'} + \theta_{n'-1}) \quad (99)$$

The accuracy of Eqs. (98) and (99) depends on the smallness of the intervals  $(\theta_n - \theta_{n-1})$ .

The sum on the right side of Eq. (87) has a singularity in the term for  $k = 0$  when  $2\mu H' \rightarrow 0$ . In the limit  $N \rightarrow \infty$ , the sum becomes an



integral and this singularity takes the form  $k^{-2}$ , where  $k$  is the distance from the origin. This type of singularity does not prevent convergence of a three-dimensional integral. For a finite sized crystal the singularity is removed by a small value of  $2\mu H^1$  (or by crystalline anisotropy) since this term corresponds to a uniform rotation of  $M$  away from the  $z$ -axis.

Since this thesis is concerned with properties of bulk materials, the sums were made to approximate the equivalent integrals. The Algol 60 computer program which was used is presented in Appendix I.

## CHAPTER IV

### BEHAVIOR WHEN MAGNETIZATION VANISHES

When the magnetization,  $M$ , vanishes, it is possible to obtain the behavior of  $M$  just below the Curie temperature,  $T_c$ , the energy remaining in the X-Y correlations at  $T_c$ , and the initial susceptibility above  $T_c$  by expanding expressions as power series of  $M$  and looking at only the first few terms. This technique is good only for  $M \ll 1$ . These results are interesting in themselves, and they serve as a check on the computer results.

In order to obtain  $M(\theta)$  as  $\theta$  goes to  $\theta_c$  (and  $\Phi_0$  goes to  $\infty$ ), the numerator and denominator on the right side of Eq.(79) are expanded in descending powers of  $\Phi_0$  to obtain

$$\langle S^z \rangle = \frac{\left[ S(S+1)/3 \right] \left[ \Phi_0^{2S-1} + (1/2)(2S-1) \Phi_0^{2S-2} + (3/10)(2S-1)(S-1) \Phi_0^{2S-3} + \dots \right]}{\Phi_0^{2S} + S \Phi_0^{2S-1} + (S/3)(2S-1) \Phi_0^{2S-2} + \dots} \quad (100)$$

The expansion is correct to three orders of  $\Phi_0$  so that the results will be correct to three orders of  $M = \langle S^z \rangle / S$ . The following algebraic equation will be used

$$(1 + aX + bX^2)^{-1} = 1 - aX + (a^2 - b)X^2 + O(X^3) \quad (101)$$

where  $O(X^3)$  indicates terms that vanish at least as fast as  $X^3$  when  $X$  goes to zero. Using Eq. (101), Eq. (100) becomes

$$\langle S^z \rangle = \left[ S(S+1)/3 \right] \left[ \Phi_o^{-1} - 1/2 \Phi_o^{-2} + a \Phi_o^{-3} + O(\Phi_o^{-4}) \right] \quad (102)$$

$$a = 3/10 - S(S+1)/15$$

The next step is to expand  $\Phi_o$  in powers of  $L = 2 \langle S^z \rangle + 2\alpha \langle S_o^+ S_\delta^- \rangle$  which is  $O(M)$  if  $\alpha$  is  $O(M)$ .

$$\Phi_o = \frac{1}{N} \sum_k \frac{1}{\exp(L(\gamma_o - \gamma_k)/\theta) - 1} \quad (103)$$

$$= \frac{\theta}{NL} \sum_k \frac{(\gamma_o - \gamma_k)^{-1}}{\left[ 1 + (1/2)(L/\theta)(\gamma_o - \gamma_k) + (1/6)(L/\theta)^2(\gamma_o - \gamma_k)^2 + O(L^3) \right]}$$

Using Eq. (101) once

$$\Phi_o = b\theta/L - 1/2 + \gamma_o L/12\theta + O(L^2) \quad (104)$$

and then using Eq. (101) again

$$\phi_o^{-1} = \frac{L}{b\theta} + \frac{L^2}{2b^2\theta^2} + \frac{L^3}{b^3\theta^3} \left[ \frac{1}{4} - \frac{b\gamma_o}{12} \right] + O(L^4) \quad (105)$$

where

$$b = \frac{1}{N} \sum_k (\gamma_o - \gamma_k)^{-1} \quad (106)$$

and since  $\sum_k \gamma_k = 0$  as can be seen from Eq. (90)

$$\gamma_o = \frac{1}{N} \sum_k (\gamma_o - \gamma_k) \quad (107)$$

Using Eqs. (102), (105), and  $M = \langle S^z \rangle / S$

$$M = \left[ (S+1)/3 \right] \left[ L/b\theta - dL^3/\theta^3 + O(L^4) \right] \quad (108)$$

$$d = (3 + \gamma_o b - 12a)/12b^3$$

It is interesting to look at the behavior of  $M$  as  $\theta$  approaches  $\theta_c$  for termination functions of the form  $\alpha(x) = \langle S^z \rangle^x / 2S^{x+1} = M^x / 2S$  for which

$$L = 2SM + S^{-1} M^x \langle S_o^+ S_\delta^- \rangle \quad (109)$$

By dropping the  $O(L^{3+})$  terms from Eq. (108) and assuming an expansion of  $\langle S_o^+ S_\delta^- \rangle$  in powers of  $M$  of the form

$$\langle S_o^+ S_\delta^- \rangle = c + eM + fM^2 + O(M^3) \quad (110)$$

the following asymptotic forms are found

$$x > 3: \quad M^2 = \frac{3\theta^2}{d(2S)^3(S+1)} \left( \frac{2S(S+1)}{3b} - \theta \right) \quad (111)$$

$x = 3$ :

$$M^2 = \frac{3bS\theta^2}{(S+1)(8bdS^4 - c\theta^2)} \left( \frac{2S(S+1)}{3b} - \theta \right) \quad (112)$$

$3 > x > 1$ :

$$M^{x-1} = -\frac{3bS}{c(S+1)} \left( \frac{2S(S+1)}{3b} - \theta \right) \quad (113)$$

$x = 1$  (if  $e = 0$ ):

$$M^2 = \frac{3bS\theta^2}{(S+1)(8bdS^4 + f\theta^2)} \left( \frac{(2S^2 + c)(S+1)}{3bS} - \theta \right) \quad (114)$$

where  $b = 0.2527$  (sc),  $0.1742$  (bcc),  $0.1122$  (fcc). The value of  $d$  which depends on the lattice type and  $S$  can be found from Eqs. (108) and (102). The values of  $c$  are given by Eq. (118). The computer

calculations for  $x = 1$  (Callen's termination) give  $M^2$  as a linear function of  $T$  from  $M = 0.4$  to  $M = 0$  implying that  $e$  in Eq. (110) is zero.

Equations (111) and (112) show that for  $x \geq 3$  the asymptotic behavior of  $M(\theta)$  as  $\theta \rightarrow \theta_c$  is given by

$$M^2 = \xi (1 - \theta/\theta_c)$$

Values of the constants  $\xi$  and  $\theta_c$  derived from Eqs. (111) and (112) are shown in Tables I and 2 in Chapter V. Figure 6 in Chapter VI shows that the computer solution for  $d(M^2)/d(\theta/\theta_c)$  approaches from below as  $M \rightarrow 0$  the value of  $\xi$  found from Eq. (112) for a face-centered-cubic lattice with  $S = 1/2$ .

For  $3 > x > 1$ , Eq. (113) implies that  $M(\theta)$  is double valued since  $\theta$  initially increases above  $\theta_c$  as  $M$  increases from zero. This behavior is also apparent from the computer solutions.

The limit of  $\langle S_o^+ S_\delta^- \rangle$  as  $M$  goes to zero can be found and yields the constant  $c$  used in the last section and the energy in the X-Y correlations at the Curie temperature. Equations (50) and (51c) combine to yield

$$\langle S_o^+ S_\delta^- \rangle = 2 \langle S^z \rangle \Phi_\delta \quad (115)$$

using the value for  $\langle S^z \rangle$  from Eq. (102), there results

$$\langle S_o^+ S_\delta^- \rangle = 2S(S+1) \Phi_\delta / 3\Phi_o + O(M) \quad (115a)$$

The function

$$\Phi_\delta = \frac{1}{N} \sum_{\mathbf{k}} \frac{e^{i\mathbf{k} \cdot \delta}}{\exp(L(\gamma_o - \gamma_{\mathbf{k}})/\theta) - 1} \quad (116)$$

can be approximated near the Curie temperature as

$$\Phi_\delta = \frac{\theta}{\gamma_o L N} \sum_{\mathbf{k}} \frac{(\gamma_{\mathbf{k}} - \gamma_o)_+^{\gamma_o}}{(\gamma_o - \gamma_{\mathbf{k}})} + O(M^0) \quad (116a)$$

$$= \frac{\theta}{\gamma_o L} \left( b - \frac{1}{\gamma_o} \right)$$

Similarly

$$\Phi_o = \frac{\theta b}{\gamma_o L} + O(M^0) \quad (117)$$

So that

$$\lim_{M \rightarrow 0} \langle S_o^+ S_\delta^- \rangle = (2/3) S(S+1) (1 - 1/b \gamma_o) \quad (118)$$

where the values of  $b$  are given in the text after Eq. (114). Values of

$\langle S_o^+ S_\delta^- \rangle / S^2$  for  $\theta = \theta_c$  are shown in Table III, Chapter VI. Equation (118)

is valid for all terminations such that  $L$  goes to zero as  $M$  goes to zero.

The initial susceptibility above the Curie point can be found by putting the  $2\mu H'$  term in Eq. (103) and expanding to first order in  $M$  and  $H'$ . If  $H = \mu H'/J$  then

$$\begin{aligned}\Phi_0 &= \frac{1}{N} \sum \frac{1}{\exp((L(\gamma_0 - \gamma_k) + 2H)/\theta) - 1} \\ &\doteq \frac{\theta}{N} \sum_k \frac{1}{L\gamma_0 + 2H - L\gamma_k} \\ &\doteq \frac{\theta \lambda(2H/L)}{L\gamma_0 + 2H}\end{aligned}\tag{119}$$

where the function  $\lambda(2H/L)$  is defined by

$$\lambda(X) \doteq \frac{1}{N} \sum_k \frac{1}{1 - \frac{\gamma_k}{\gamma_0 + X}}\tag{120}$$

A table of values of  $\lambda(X)$  is contained in Appendix II.

To the first order for all terminations  $\alpha(x)$  with  $x > 1$ ,  $L$  is  $2SM$ . From Eqs. (102) and (119) to first order in  $M$

$$M = \frac{(S+1)(2SM\gamma_0 + 2H)}{3\theta \lambda(H/SM)}\tag{121}$$



If a relative inverse susceptibility,  $\chi^{-1}$ , is defined by

$$\begin{aligned}\chi^{-1} &= \frac{\mu H'}{2SJM} \\ &= \frac{H}{2SM}\end{aligned}\tag{122}$$

then Eq. (121) can be written

$$\chi^{-1} = \left[ 3\lambda(2\chi^{-1})/4S(S+1) \right] \theta - \gamma_o/2 \tag{123}$$

The behavior of the susceptibility can be understood by writing Eq. (123) for  $S = 1/2$  and using the Weiss-Law Curie point,  $\theta_w = \gamma_o/2$ .

$$\chi^{-1} = \lambda(2\chi^{-1})\theta - \theta_w \tag{124}$$

$$\lambda(\infty) = 1$$

$$\lambda(o) = 1.5164 \text{ (sc)}$$

$$= 1.3932 \text{ (bcc)}$$

$$= 1.3447 \text{ (fcc)}$$

If  $\lambda(2\chi^{-1})$  were always unity, Eq. (124) would agree with the Weiss molecular field model results. As it is, the Weiss law is a lower

limit of  $\chi^{-1}$  which is approached asymptotically as  $\theta$  and  $\chi^{-1}$  become increasingly large as is shown in Fig. 8 in Chapter VI. The values of  $\lambda(o)$  were obtained by Watson who put Eq. (120) in the form of an elliptic integral.<sup>34, 35</sup>

The susceptibility given by Eq. (124) agrees with the results from direct computation (Figs. 7 and 8). Also since  $\lambda(o) = b\gamma_o$  the Curie points implied by Eq. (123) agree with those implied by Eq. (112).

## CHAPTER V

### CHOOSING THE TERMINATION FUNCTION

The formalism has been developed up to this point for an arbitrary termination function,  $\alpha$ . Results for a set of functions,  $\alpha(x)$  were derived in the last chapter, but in order to choose the proper function  $\alpha$ , one must go outside of the Green function formalism to compare with results of other solutions of the Heisenberg model and experiment.

Looking back at Eqs. (94) and (95) it is apparent that the sums  $\Phi_j$  depend uniquely on  $R$  ( $R = k_B T/JL$ ) and the reduced magnetic field  $H$ , ( $H = \mu H'/J$ ). Therefore  $\langle S^z \rangle$ ,  $\langle S_o^+ S_j^- \rangle$ , and all other expectation values are functions of  $R$  and  $H$ . The termination function's role is in the relation between  $R$  and the reduced temperature  $\theta$  ( $\theta = k_B T/J$ ) which is

$$\theta = R(2 \langle S^z \rangle + 2 \alpha \langle S_o^+ S_\delta^- \rangle) \quad (125)$$

The assumption is made that  $\alpha$  is a function only of  $\langle S^z \rangle$ . This is reasonable since for a fixed value of applied field, the functions  $R$ ,  $\langle S_o^+ S_j^- \rangle$ , and  $\Phi_j$  are all functions of  $\langle S^z \rangle$ . Equations (50) and (89) show that  $\Phi_o$  is a monotonic function of  $\langle S^z \rangle$  and Eq. (95) shows that  $\Phi_o$  is

also a monotonic function of  $R$ ; therefore,  $R$  is a monotonic function of  $\langle S^z \rangle$ . All expectation values are functions of  $R$  and hence are functions of  $\langle S^z \rangle$ . The variables  $H$ ,  $S$ , and lattice structure are contained implicitly in  $\langle S^z \rangle$ .

There is no unique means for determining  $\alpha$ ; however, there follows a number of arguments that indicate the best choice is  $\alpha(x = 3)$  or

$$\alpha = \langle S^z \rangle^3 / 2S^4 \quad (126)$$

The Heisenberg model is probably a very good model for an insulating ferromagnet such as EuO where the Eu atoms are on a face-centered-cubic lattice and seem to have a magnetic moment of 7 Bohr magnetons indicating  $S = 7/2$ . If the  $M$  vs.  $T$  curve measured for EuO (Ref. (42)) is assumed to represent a Heisenberg ferromagnet, then  $\alpha$  could be determined over the whole range of  $0 \leq \langle S^z \rangle \leq S$  by using Eq. (125) and values of  $R$  as a function of  $\langle S^z \rangle$  as computed by the Green function formalism. As shown in Fig. 1, the function  $\alpha$  given by Eq. (126) produces the correct magnetization curve.

The values of the reduced Curie temperature,  $\theta_c$ , for various termination functions, can be compared with the values obtained by high temperature series solutions for the Heisenberg model.<sup>11</sup> This is done in Table 1. The result of this comparison is that the functions  $\alpha(x)$  with

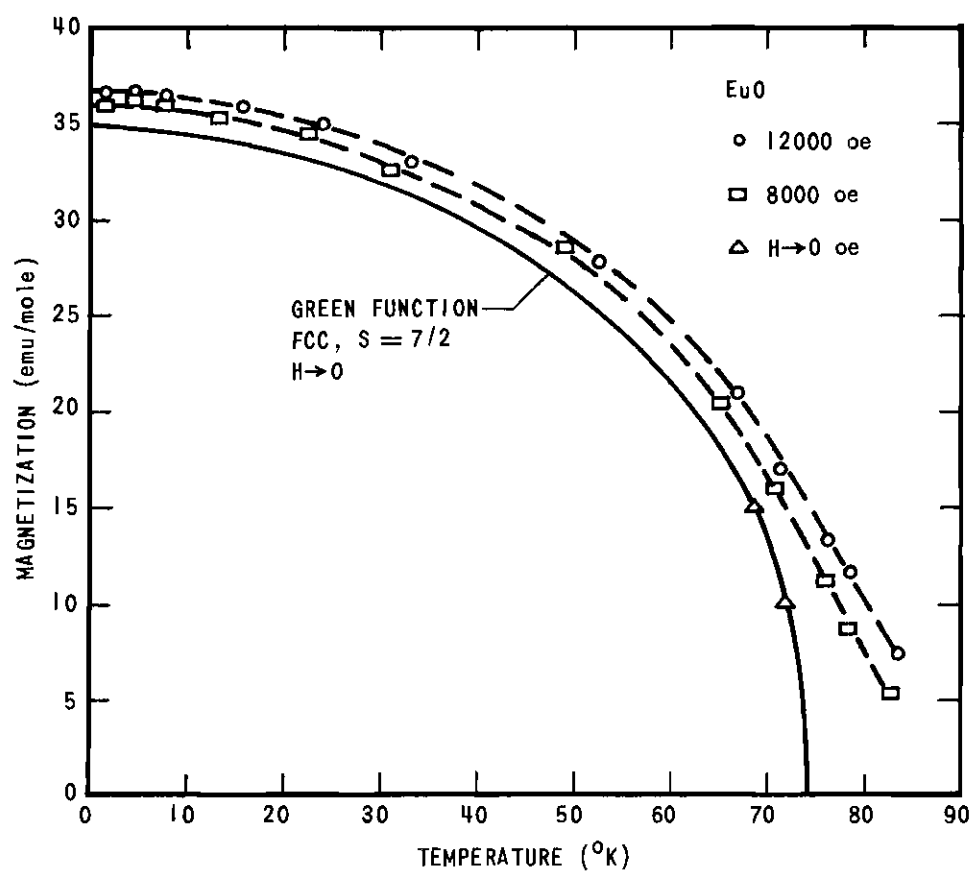


Figure 1. The magnetization of EuO as measured by Matthias, Bozorth, and Van Vleck compared with a theoretical curve calculated by using the Green function technique.

$x \geq 3$ , which all give the same Curie point, give better agreement with the  $(1/T)$  series results than  $\alpha(1)$ . The functions with  $x < 1$  are ruled out because they do not produce a transition and the function with  $1 < x < 3$  are ruled out because they imply a first order transition.

Table 1. Curie Temperatures Given by Use of Two Different Termination Functions in Green Function Formalism Compared with High Temperature Expansion Results

	$\frac{3k_B T_c}{4S(S+1)J}$		
Calculation	$S = 1/2$	$S = 1$	$S = \infty$
Simple-cubic ( $\gamma_0 = 6$ )			
Present work ( $x = 3$ )	2.0	2.0	2.0
Callen ( $x = 1$ )	2.7	2.4	-
$(1/T)$ Series	2.0	2.2	2.4
Body-centered-cubic ( $\gamma_0 = 8$ )			
Present work ( $x = 3$ )	2.9	2.9	2.9
Callen ( $x = 1$ )	3.7	3.4	-
$(1/T)$ Series	2.7	2.9	3.2
Face-centered-cubic ( $\gamma_0 = 12$ )			
Present work	4.5	4.5	4.5
Callen	5.6	5.3	4.9
$(1/T)$ Series	4.0	4.4	4.8

Another comparison can be made with the behavior of  $M$  as a function of  $H$  at the Curie temperature. Kouvel and Fisher<sup>9</sup> have analyzed data for Nickel<sup>23</sup> and have shown that at the Curie point.

$$M \propto H^{0.24} \quad (\theta = \theta_c) \quad (127)$$

They also point out that the applied field,  $H$ , and magnetization,  $M$ , of a ferromagnetic system are thermodynamically isomorphic with the pressure and density of a gas. The Curie point of the magnetic system is analogous with the critical point of a gas where the density,  $\rho$ , and the pressure,  $P$ , obey the following relation

$$|P - P_0| = c |\rho - \rho_0|^\tau$$

At the critical point of Xe, CO<sub>2</sub>, and H<sub>2</sub> the exponent,  $\tau$ , is 0.24 or 0.25.<sup>25</sup>

Using the  $\alpha(x=3)$  termination function,  $M(H)$  at  $\theta = \theta_c$  was calculated for  $H = 125; 100; 4160; 10,000$  oe (see Figs. 2, 3). Agreement with the experimental data for nickel was obtained with a value for  $\mu$  of 0.642 Bohr magnetons. The value  $\mu = 0.642 \mu_B$  was deduced by Kouvel and Fisher<sup>9</sup> by comparing the behavior of the susceptibility of nickel above the Curie temperature with Domb and Sykes' results from high temperature series expansions for a Heisenberg ferromagnet with spin 1/2.

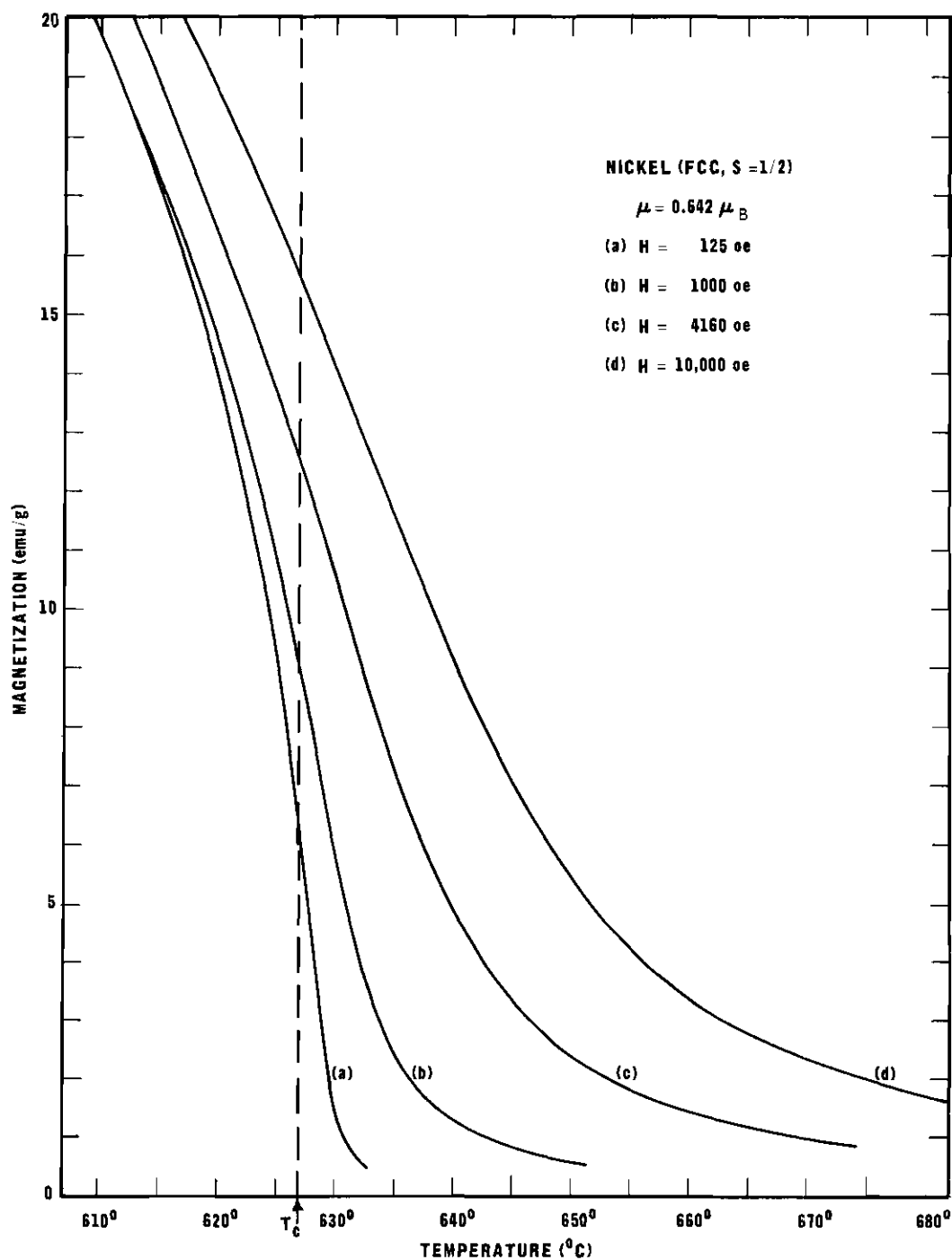


Figure 2. Theoretical magnetization curves in the vicinity of the Curie point for four values of applied field. The scales correspond to nickel. The calculations were for a  $60 \times 60 \times 60$  face-centered-cubic lattice with spin equal to  $1/2$ .



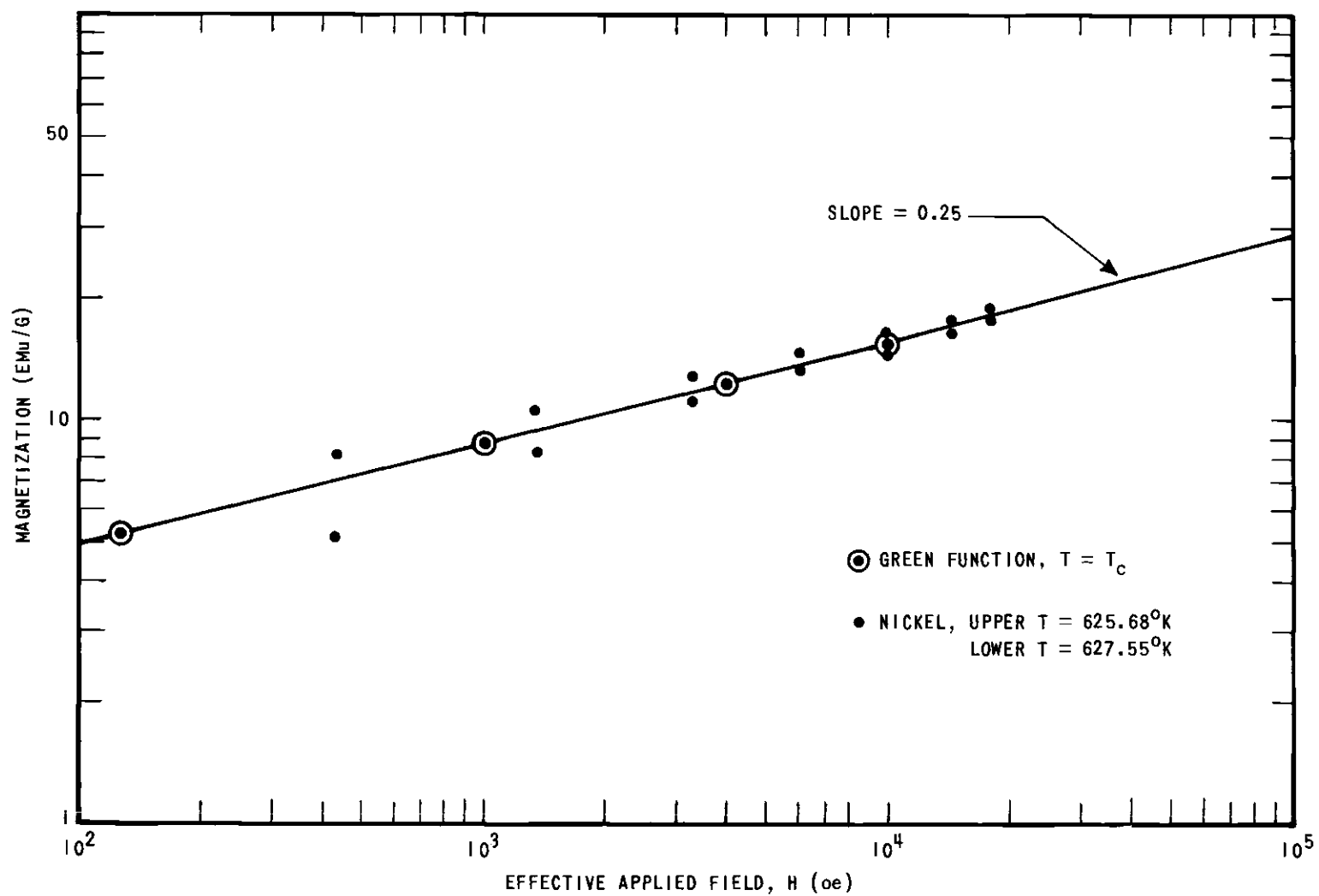


Figure 3. Magnetization as a function of applied field,  $H$ , at the Curie temperature. The theoretical points were taken from the curves shown in Figure 2. The experimental points were measured by Weiss and Forrer.

The limit of  $dM^2/d(T/T_c)$  as  $M$  vanishes,  $\xi$ , is very sensitive to the termination function. The value of  $\xi$  for  $\alpha(x=3)$  for a face-centered-cubic lattice for  $S = 1/2$  from Eq. (112) is 5.19, which is much higher than the value 2.23 for  $\alpha(x > 3)$  and the value for  $\alpha(x=1)$  indicated by computer results of about 1.7. The Weiss and Forrer data<sup>23</sup> shown in Fig. 6 indicates that  $\xi$  is about 5.6 for nickel. Belov<sup>37</sup> reports a value of 6.7 for nickel. These results are shown in Table 2.

Table 2. Results for a F. C. C. Lattice with Spin 1/2 for Termination Functions of the Type:  $\alpha(x) = \langle S^z \rangle^x / 2S^{x+1}$

Function	$k_B T_c / J$	$\xi = \lim_{M \rightarrow 0} \frac{M^2}{1 - T/T_c}$	Comments
$0 \leq x < 1$	$\infty$	-	$x = 0$ same as Hartree-Fock
1	5.6	1.7	Callen's function <sup>19</sup>
$1 < x < 3$	4.5	-	$M(T)$ double valued
3	4.5	5.2	Present function
$3 < x \leq \infty$	4.5	2.3	$x = \infty$ same as Tyablikov <sup>14</sup>
Experiment	-	5.6 - 6.7	Weiss-Forrer <sup>23</sup> and Belov <sup>37</sup>

In general, the results of calculations using  $\alpha(x=3)$ , Eq. (126), have shown good agreement with experimental results from EuO and

nickel and the results of high temperature solutions for the Heisenberg model. More of these results are discussed in the next chapter.

## CHAPTER VI

### GENERAL RESULTS

All of the results of the calculations are given in terms of the dimensionless quantities  $\theta$ ,  $M$ ,  $H$  defined by

$$\theta = k_B T/J \quad (130)$$

$$M = M'/(2 \eta \mu S) \quad (131)$$

$$H = 2 \mu H' / J \quad (132)$$

where  $T$  is the temperature in degrees Kelvin,  $H'$  is the applied field in oersteds, and  $M'$  is the magnetization per unit weight or per unit volume depending on whether  $\eta$  is the number of atoms per unit weight or per unit volume.

The lattice type and density of a real material are easily determined from non-magnetic measurements; however, values of the exchange constant,  $J$ , the spin per lattice site,  $S$ , and the magnetic moment,  $\mu$ , per atom per unit of spin,  $\hbar/2$ , generally require comparison with a particular theory. Since the actual Curie temperature,  $T_c$ ,

of most materials is known,  $J$  can be determined by

$$J = k_B T_c / \theta_c \quad (133)$$

where  $\theta_c$  depends on the theory used for comparison. The step indicated by Eq. (133) is implied when comparisons are made on the basis of a reduced temperature scale ( $T/T_c$ ). When the comparison is between theoretical results, as in Fig. 4, the implication is that a different value of  $J$  for each theory has been used. For real materials there may be small changes in  $J$  at high temperatures due to lattice expansion or changes in the conduction band occupation.

The magnetic moment,  $\mu$ , can be determined at low temperatures where  $M = 1$  by using Eq. (131). The value of  $\mu$  for nickel from this method for  $S = 1/2$  is  $0.606 \mu_B$ , while the value which best agrees with the Heisenberg model at temperatures around the Curie point is  $0.642 \mu_B$ .<sup>9</sup> The magnetic moment of a free electron,  $\mu_B$ , can be reduced in a crystal by a mixing of  $S^z$  states by the crystalline field and by a negative magnetic polarization of the conduction electrons.<sup>26, 27</sup> Neutron diffraction experiments may eventually determine whether the apparent change in the magnetic moment is a real effect or whether it is a deficiency of the Heisenberg model when applied to nickel.<sup>28, 29, 30</sup> Figure 4 shows the magnetization curve for nickel compared to the theoretical curves for  $\mu = 0.606 \mu_B$  and  $\mu = 0.642 \mu_B$  from the present

calculations on a  $T/T_c$  temperature scale. The results of using Callen's termination function,  $\alpha(x=3)$ , with  $\mu = 0.606\mu_B$  is also shown for comparison. The magnetization curves for a b. c. c. lattice with  $S = 1$  is compared with iron in Fig. 5.

Equation (112), which was derived by taking the first two non-zero terms in a power series expansion of  $M$ , showed that as  $M$  approaches zero,  $M^2$  approaches  $\xi(1 - (T/T_c))$  where  $\xi$  is 5.2 for a f. c. c. lattice with  $S = 1/2$ . Figure 6 shows  $d(M^2)/d(T/T_c)$  derived by the calculations for a f. c. c. lattice with  $S = 1/2$  and the values for nickel measured by Weiss and Forrer. The curves show that  $d(M^2)/d(T/T_c)$  approaches  $\xi$  only as  $M$  approaches zero. The decrease in  $d(M^2)/d(T/T_c)$  is very rapid when plotted on a  $(T/T_c)$  scale since  $M = 0.1$  corresponds to a value of  $(T/T_c)$  about 0.998.

The inverse initial susceptibility,  $\chi^{-1}$ , calculated from Eq. (123) is shown in Fig. 7 in units that correspond to nickel. Also shown are values of  $H/M$  for four values of  $H$  calculated using Eqs. (51), (87), and (88). The inverse susceptibilities calculated by the Green function equations are lower than the experimental points<sup>9</sup> for nickel but approach the experimental values as the temperature increases. Also the calculated susceptibilities vary proportional to  $(T - T_c)^2$  near the Curie point instead of  $(T - T_c)^{4/3}$  as predicted by high temperature series for the Heisenberg ferromagnet<sup>11</sup> and as is observed for nickel<sup>9, 31</sup> and iron.<sup>12</sup>

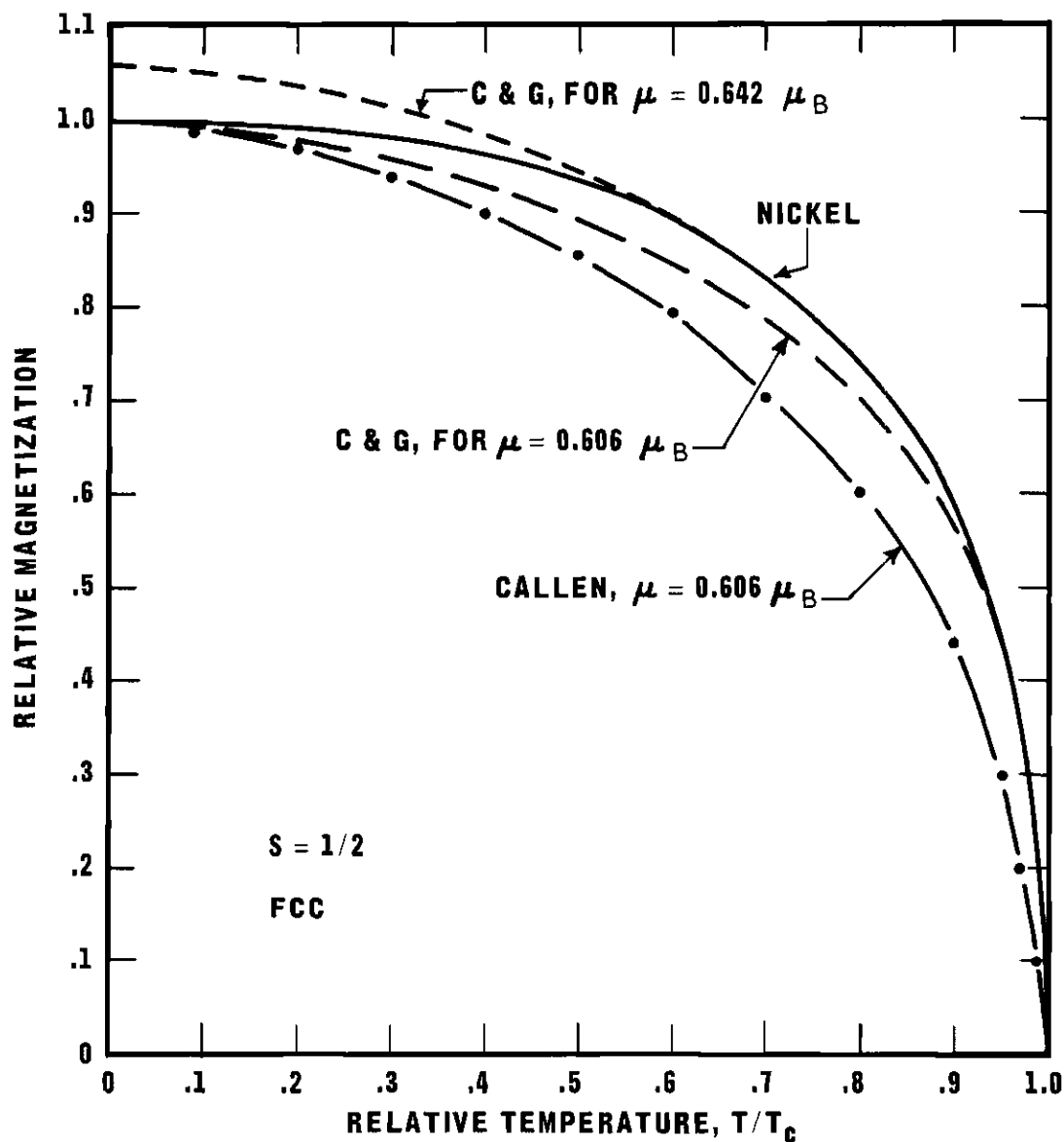


Figure 4. The magnetization curve for nickel compared with three theoretical curves. The curves marked C & G were calculated using the present termination function and the two values for the magnetic moment. The curve marked Callen was made using Callen's original termination function.

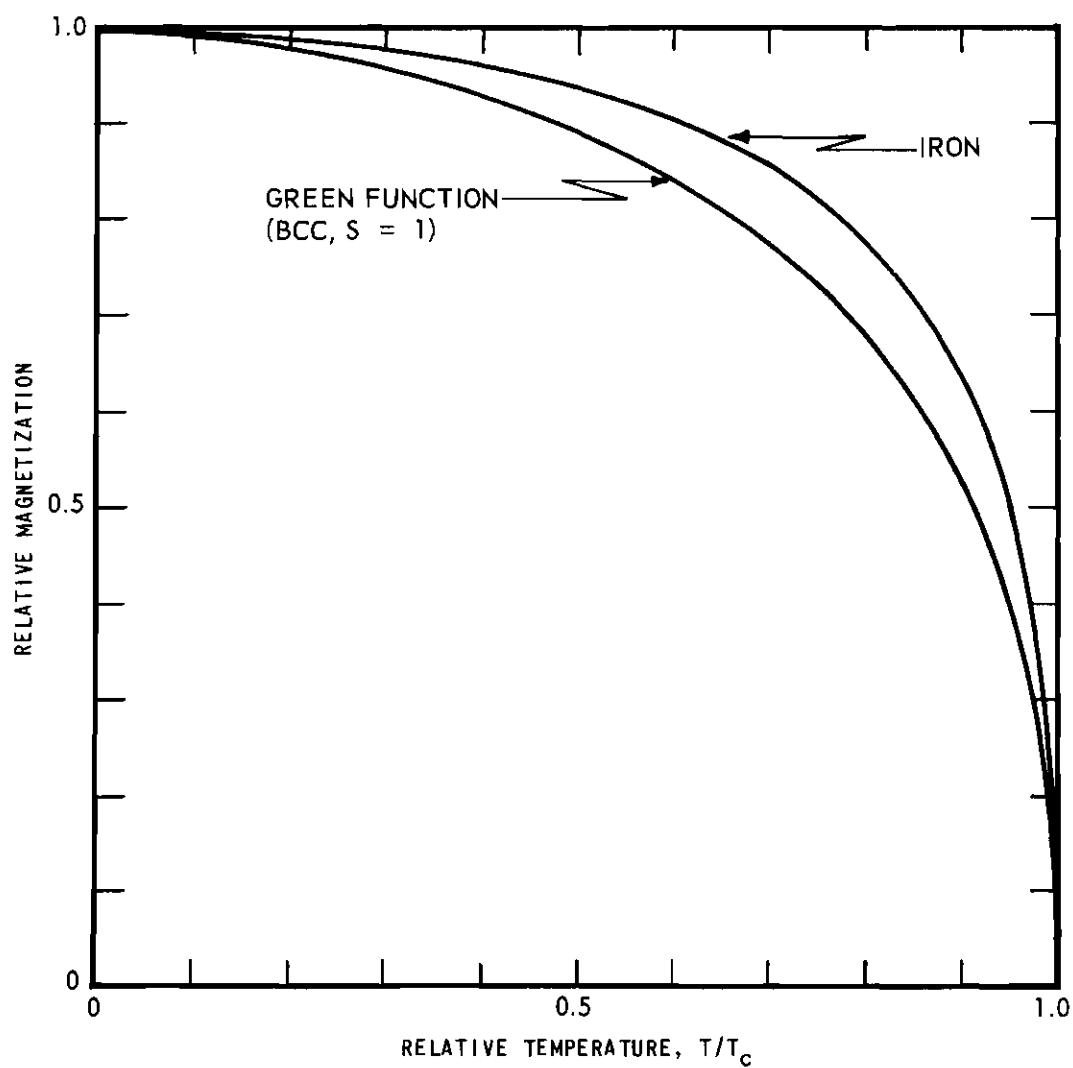


Figure 5. Magnetization curve for iron compared with theoretical curve for a body-centered-cubic lattice with spin equal to one.



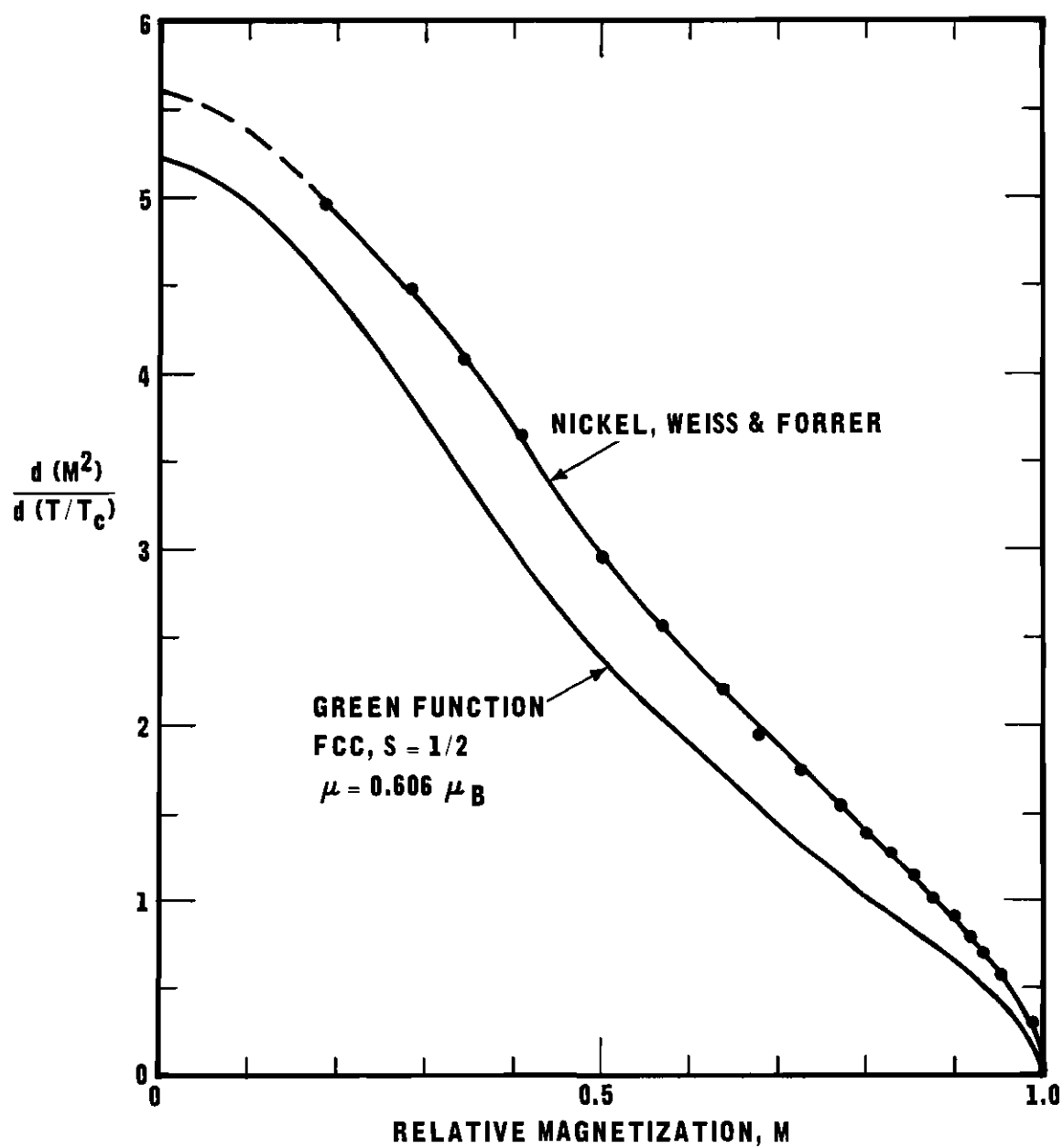


Figure 6. Derivative of the square of the relative magnetization with respect to the relative temperature from Weiss and Forrer's data and from the Green function equations.

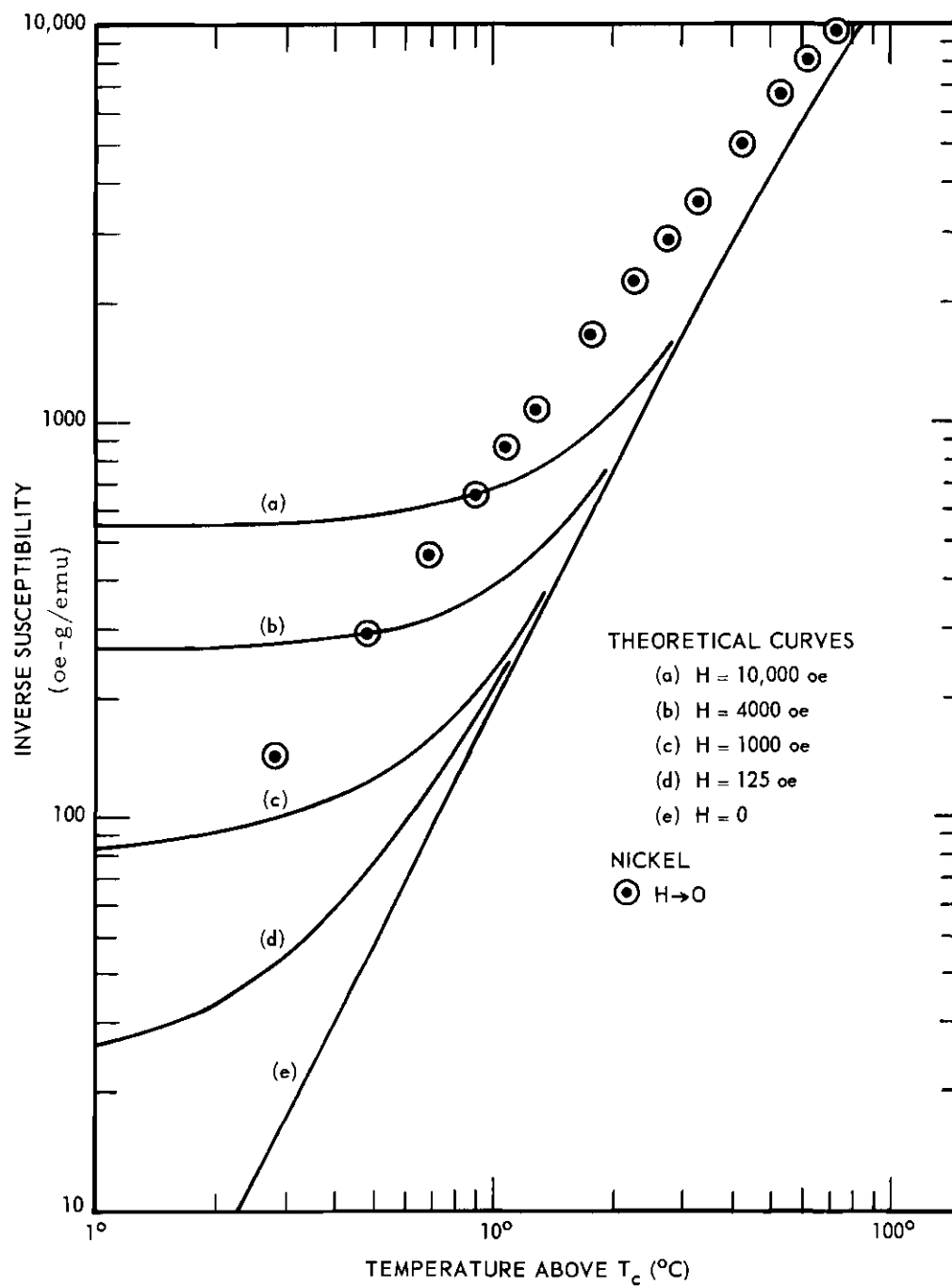


Figure 7. Calculated inverse susceptibilities for a face-centered-cubic lattice with spin equal to  $1/2$  and experimental values for nickel. The units for the theoretical values were derived using  $\mu = 0.642 \mu_B$  and  $T_c = 627.2^\circ \text{K}$ .

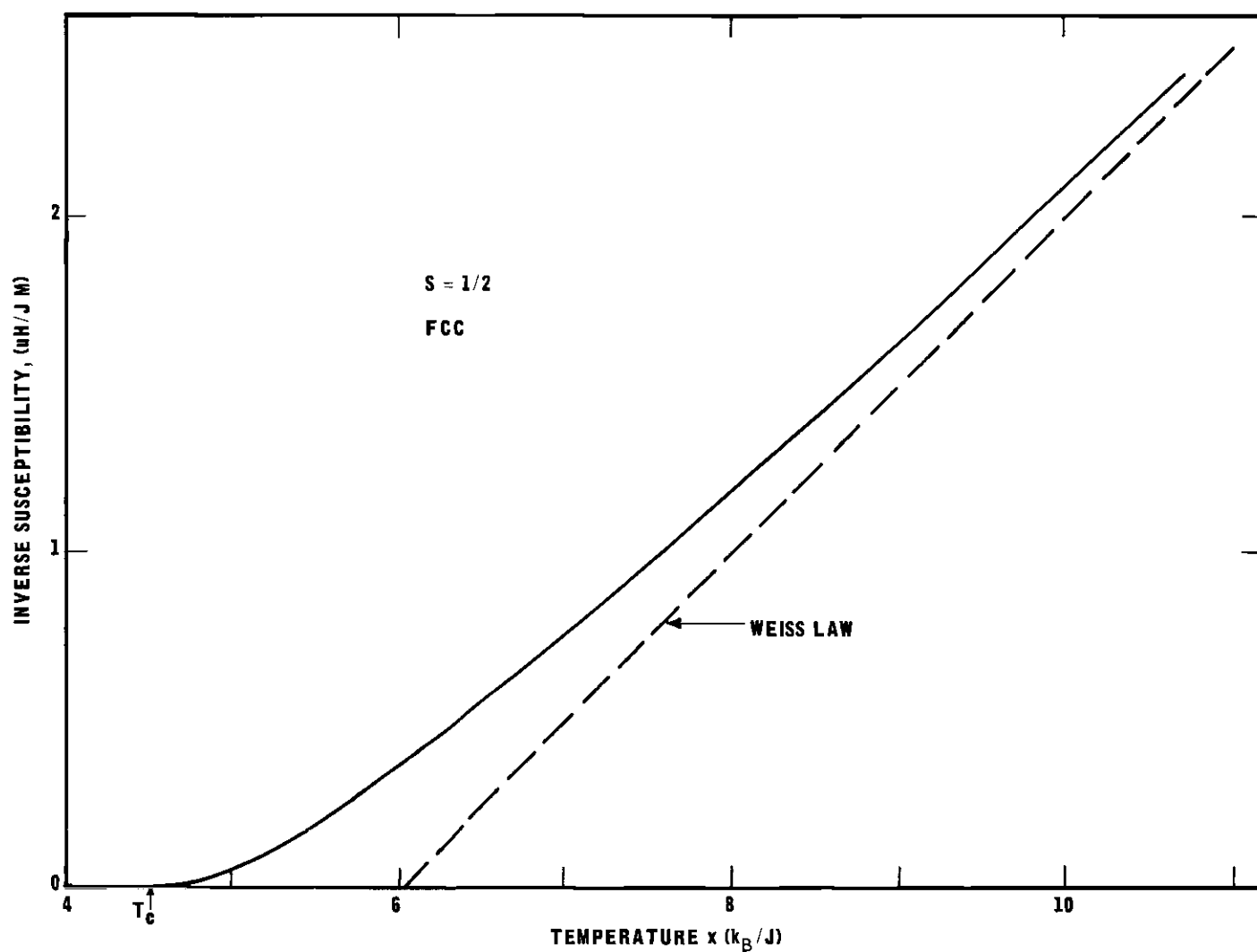


Figure 8. The inverse susceptibility versus temperature showing asymptotic convergence to the Weiss molecular field result.

The calculated exchange energy of a face-centered-cubic,  $S = 1/2$ , Heisenberg ferromagnet is shown in Fig. 9. The portions of the energy due to nearest neighbor Z component correlations and X-Y components are also shown. At zero temperature there is maximum correlation between the nearest neighbor Z components since all the spins are in  $+1/2$  eigenstates of  $S^z$ . As the temperature increases the portion of the energy due to the Z component correlations decreases approximately like  $M^2$ ; however, this decrease is almost compensated by the increase in X-Y component correlations for temperatures up to about half  $T_c$ . At  $T_c$ , the Z component nearest neighbor correlations disappear, the energy due to the X-Y nearest neighbor correlations rises rapidly to 51 per cent of the maximum energy, then decreases above  $T_c$ , and the total exchange energy has an inflection point. Above  $T_c$ , the exchange energy is entirely due to X-Y correlations between nearest neighbors which disappear asymptotically as  $T$  increases.

The specific heat of a Heisenberg ferromagnet found by a high temperature series expansion has been integrated over  $T$  from  $T_c$  to  $\infty$  by Domb and Sykes.<sup>11</sup> The result for  $S = 1/2$  was that approximately 45 per cent of the exchange energy remains at  $T_c$ , which is reasonably close to the 51 per cent value predicted by the Green function theory. A more thorough comparison is made in Table 3 using values from Eq. (118).

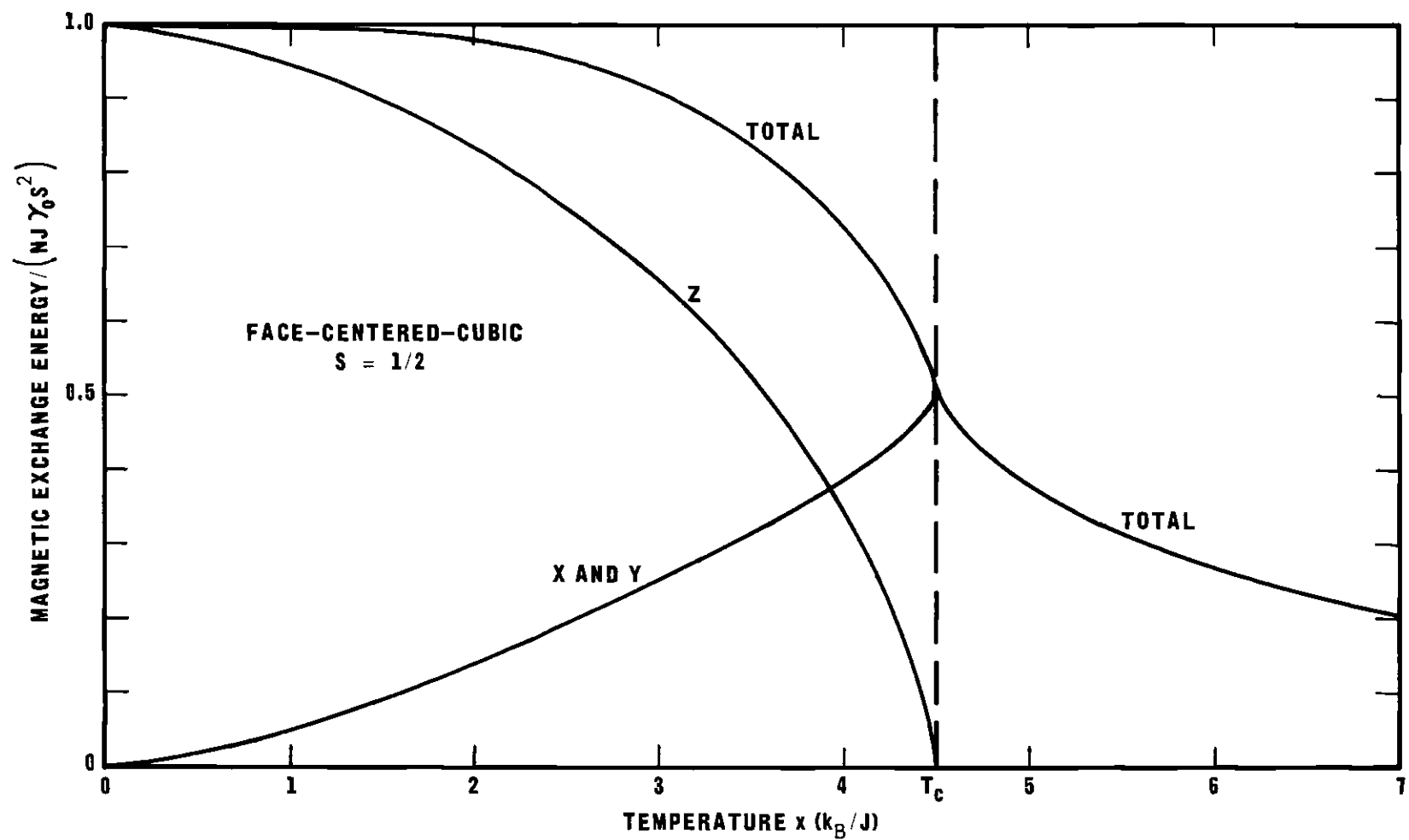


Figure 9. The relative magnetic energy of a face-centered-cubic lattice with  $S = 1/2$ . The component due to the  $S_o^z S_\delta^z$  correlations and the component due to  $S_o^x S_\delta^x$  and  $S_o^y S_\delta^y$  correlations are also shown.

Table 3. Fraction of the Exchange Energy Present at the Curie Point

Calculation	$S = 1/2$	$S = 1$	$S = 2$	$S = \infty$
Green Function				
Simple-cubic	0.68	0.45	0.34	0.23
Body-centered	0.56	0.38	0.23	0.19
Face-centered	0.51	0.34	0.26	0.17
(1/T) Series	0.45	0.34	-	0.19

The specific heat given by the derivative of the total exchange energy shown in Fig. 9 is presented in Fig. 10 with units derived by using the Curie temperature and atomic weight of nickel. The dotted curve was obtained by Bozorth by subtracting from the total specific heat of nickel the components due to lattice vibrations, expansion, and conduction electrons. The agreement between the Green function theory and the experimental values of specific heat is quite good, perhaps because the comparison is independent to the magnetic parameter  $\mu$ .

The entropy corresponding to the energy and specific heat curves of Figs. 9 and 10 is shown in Fig. 11. The maximum value of the entropy of a system of  $N$  particles with two states is  $Nk_B \ln(2)$ . At the Curie temperature, the calculated entropy for the  $S = 1/2$ , f.c.c. system

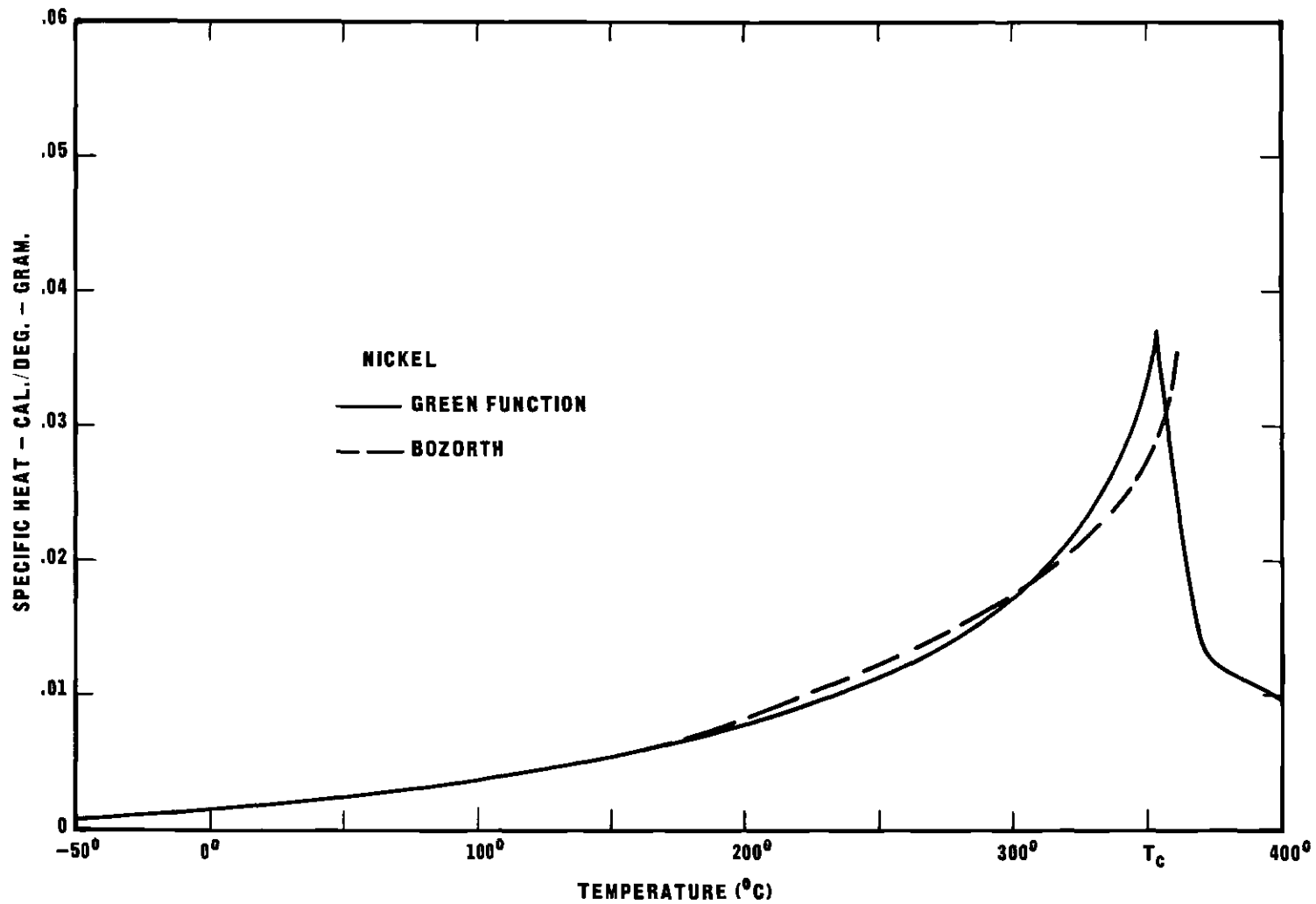


Figure 10. The specific heat of a face-centered-cubic lattice with  $S = 1/2$ . The scales have been fitted to the atomic weight and Curie temperature of nickel so that a comparison can be made with Bozorth's estimate of the magnetic specific heat of nickel.

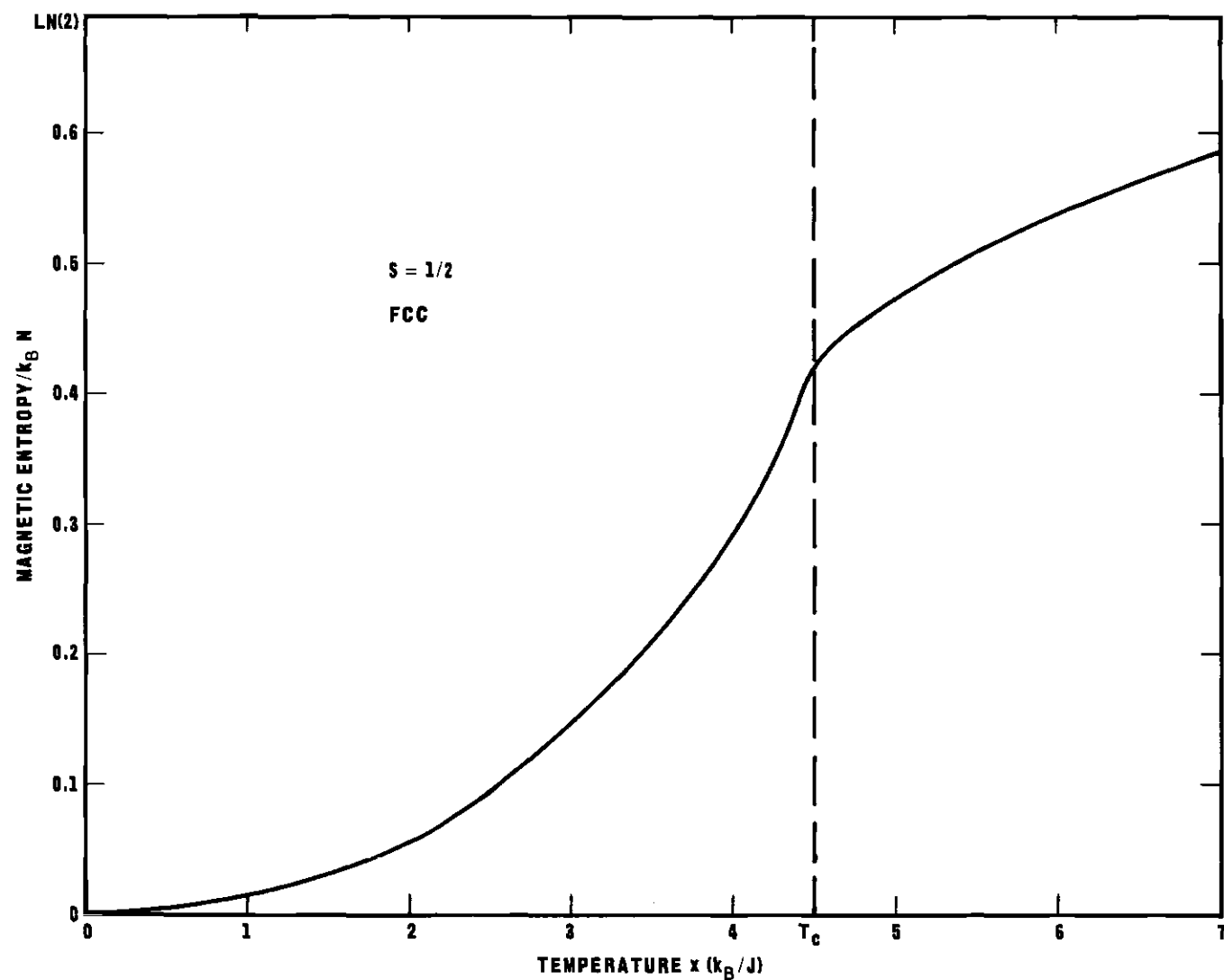


Figure 11. The entropy of a face-centered-cubic lattice with spin  $1/2$ . The limiting value for the entropy as temperature increases is  $Nk_B \ln(2)$ .



is  $0.44 k_B N$  which is 64 per cent of the limiting value. The corresponding value calculated by high temperature series is 60 per cent.<sup>11</sup>

The effect of temperature on the energies  $E_k$  is to multiply them by a renormalization factor,  $(\langle S^z \rangle + \alpha \langle S_o^+ S_\delta^- \rangle) / S$  which reduces the effective value of the exchange constant. The renormalization factor can be measured by inelastic neutron diffraction.<sup>39</sup> Figures 12 and 13 show the calculated renormalization factors for a face-centered-cubic lattice with  $S = 1/2$  and for a body-centered-cubic lattice with  $S = 1$  and the results from experiments on nickel and iron by Lowde.<sup>38</sup>

The correlation function  $\langle S_o^+ S_j^- \rangle$  can be calculated using the Green function technique. As can be seen from Fig. 14 the correlation function increases for all values of  $j$  as the temperature increases up to the Curie temperature, then decreases rapidly. If the function  $\langle S_o^+ S_j^- \rangle$  is normalized by dividing by  $\langle S_o^+ S_o^- \rangle$  and plotted versus  $j$  for several fixed temperatures the following behavior is observed (Fig. 15). At  $T = 0$  the correlation is infinite since the first reversed spin is in a plane-wave distribution state. At  $T = 0.05 T_c$  the normalized correlation function is down to 0.1 at  $j = 5$  lattice spacings and decreases almost exponentially with  $j$ . At  $T = T_c$ , the renormalized function is down to 0.05 at  $j = 2$  and at  $T = 1.13 T_c$ , it is down to 0.01 at  $j = 2$ . These results are consistent with the picture of the reversed spins being in plane-wave states at low temperatures (spinwaves) and localized states at high temperatures where the Weiss theory and BPW results are valid.

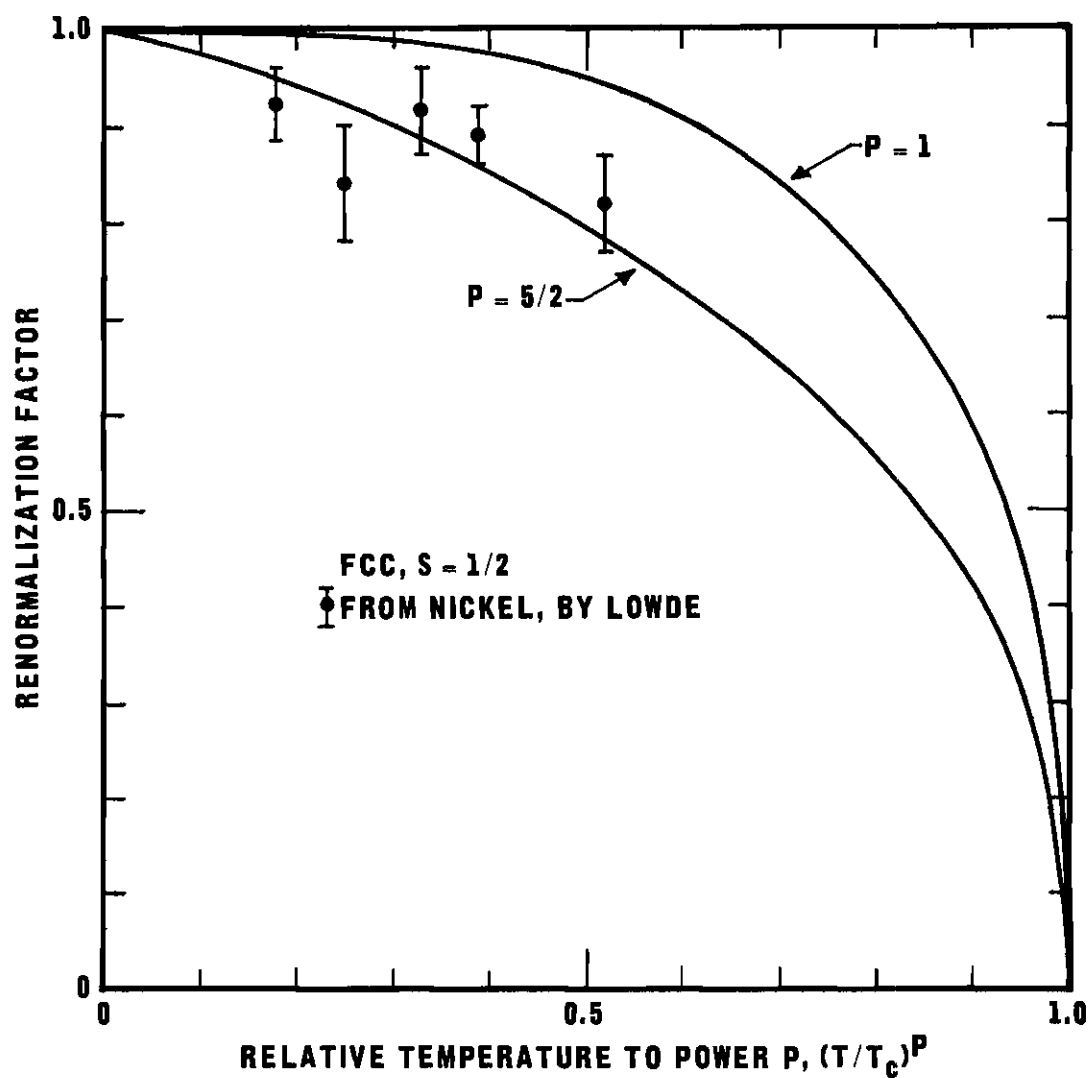


Figure 12. The renormalization factor for a face-centered-cubic lattice plotted versus the relative temperature to the first power and to the 5/2 power. The experimental results by Lowde are plotted versus the 5/2 power scale.

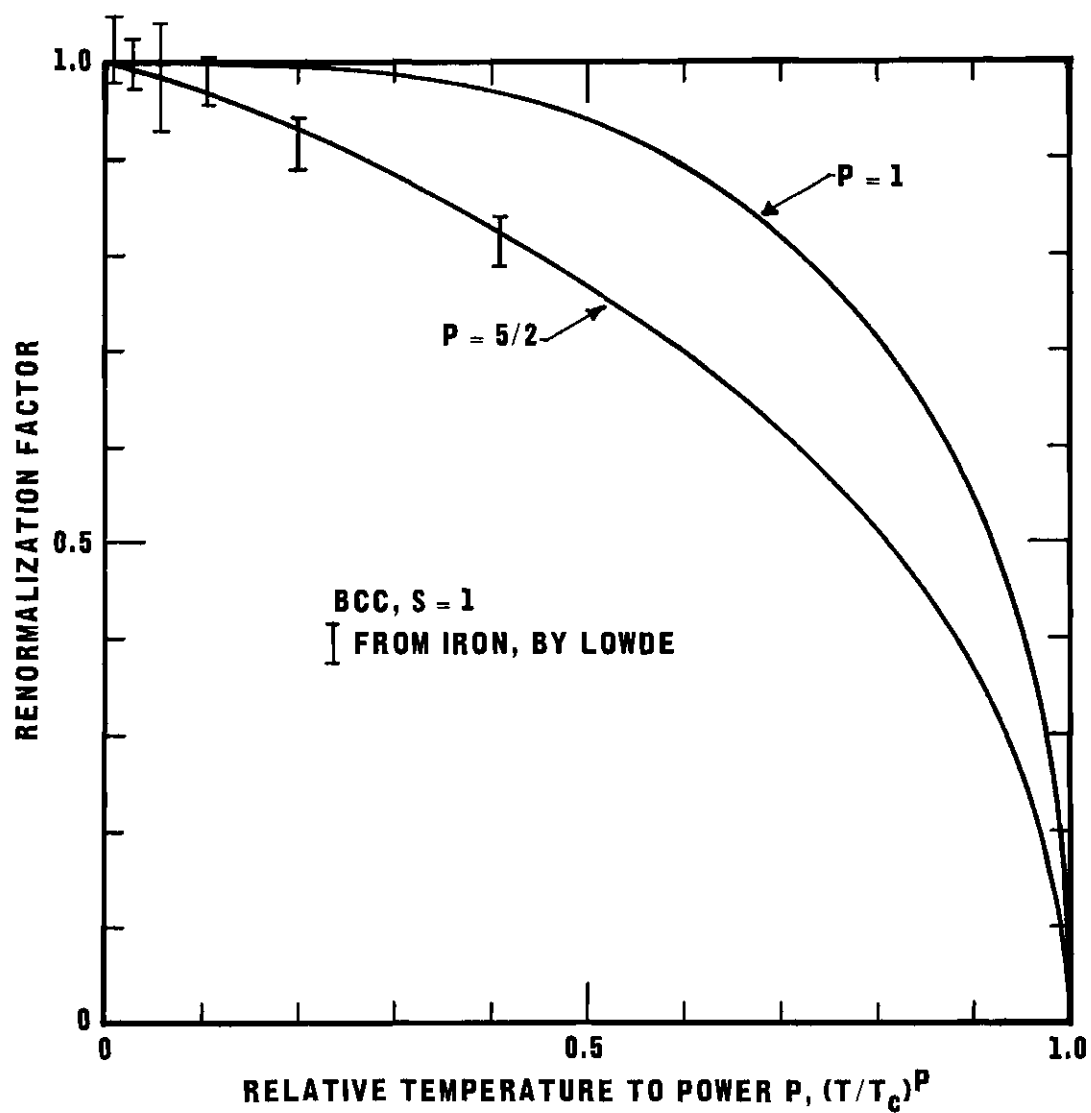


Figure 13. The renormalization factor for a body-centered-cubic lattice plotted versus the relative temperature to the first power and to the 5/2 power. The experimental results by Lowde are plotted versus the 5/2 power scale.

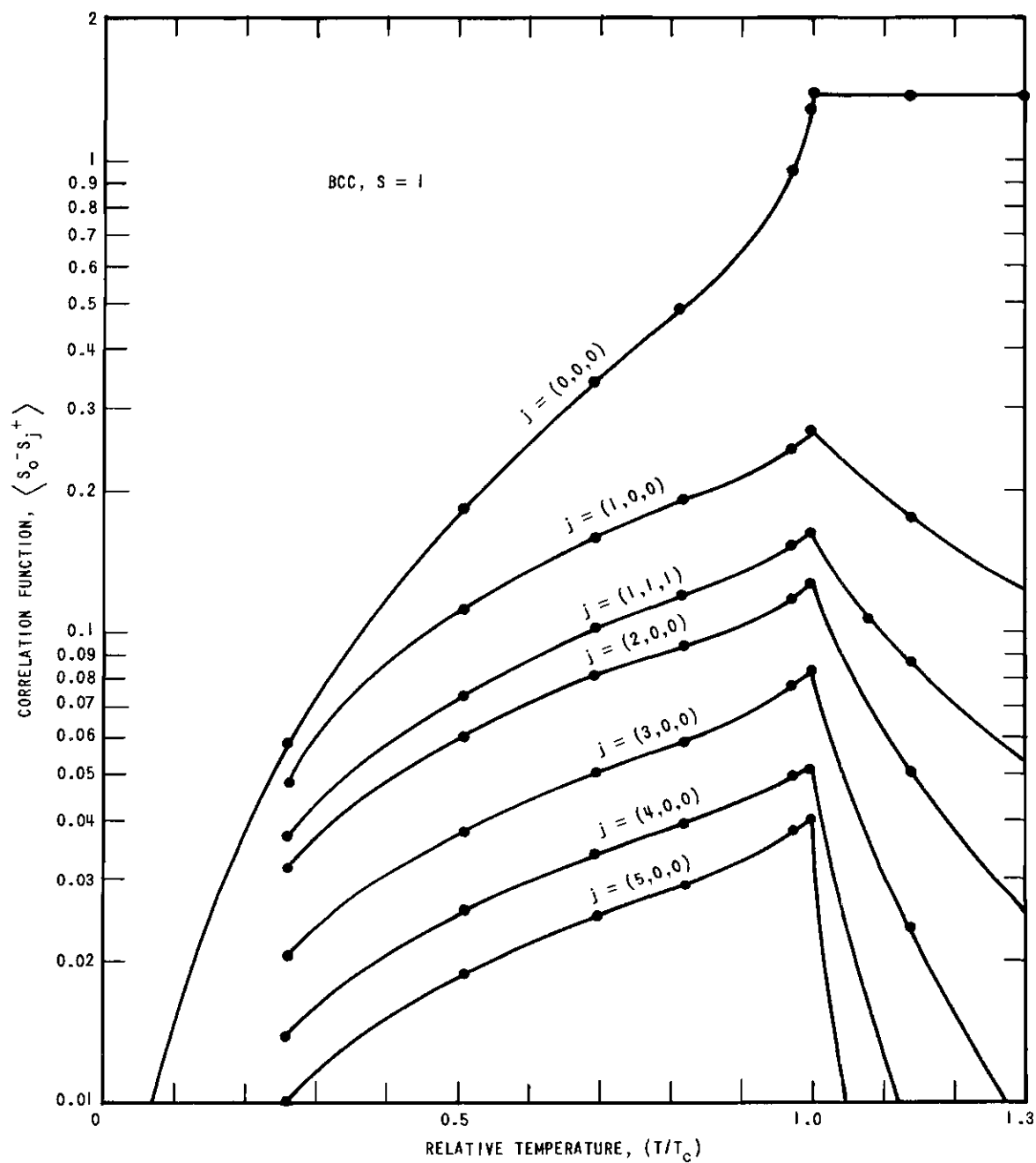


Figure 14. The spin-spin correlation function  $\langle S_0^+ S_j^- \rangle$  on a logarithmic scale versus the relative temperature. It should be noted that  $\langle S_0^+ S_j^- \rangle = \langle S_j^- S_0^+ \rangle$  except when  $j = 0$ . The points were computed for a  $60 \times 60 \times 60$  lattice with magnetization in the  $-z$  direction.

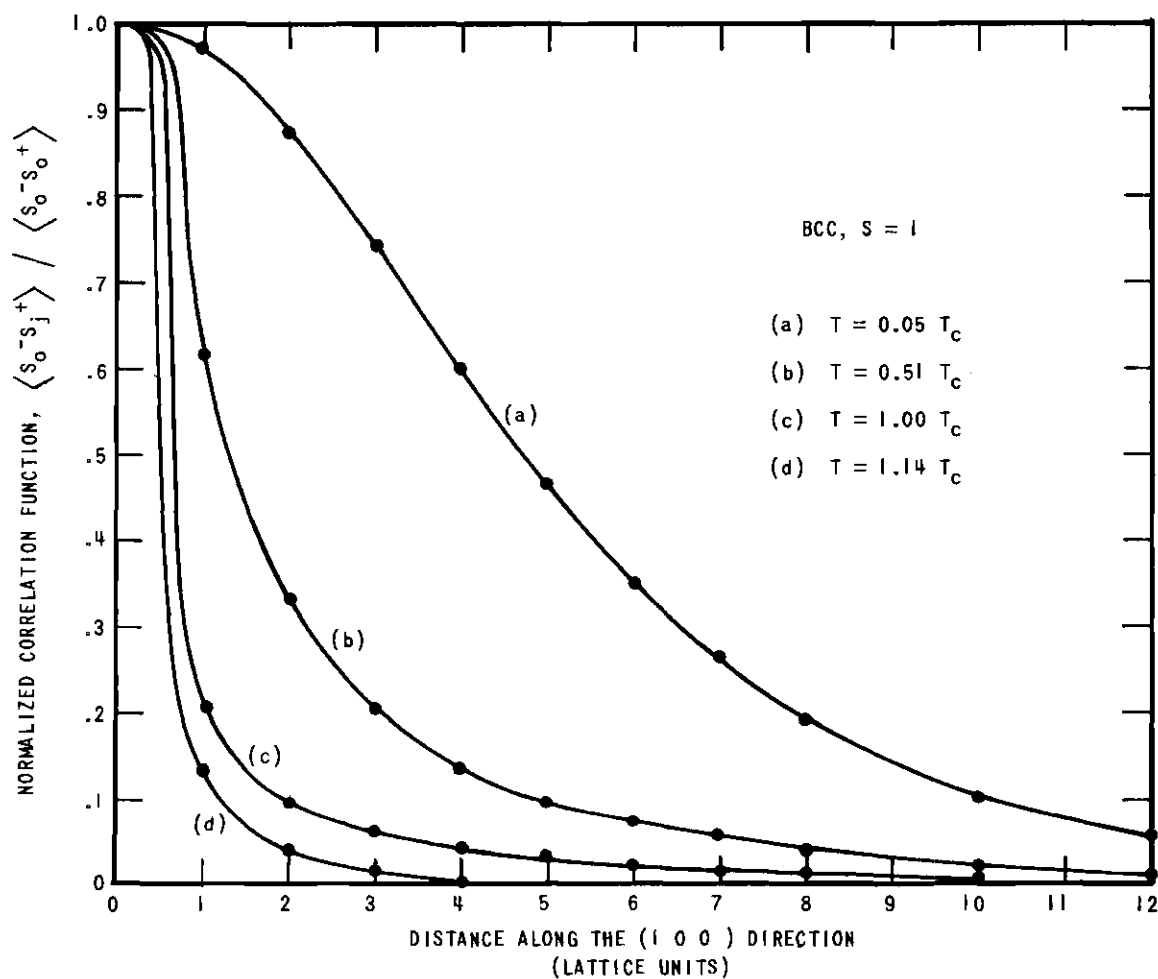


Figure 15. The spin-spin correlation function  $\langle S_0^+ S_j^- \rangle$  normalized to one for  $j = 0$  for four temperatures versus the distance in lattice spacings along the  $(100)$  direction. The points were computed for a  $60 \times 60 \times 60$  lattice with magnetization in the  $-z$  direction.

The Fourier transform of the correlation function,  $F(k)$ , is defined by

$$F(\vec{k}) = \sum_j \langle S_o^+ S_j^- \rangle e^{ij \cdot k} \quad (134)$$

which from Eqs. (50) and (3a) is given by

$$F(\vec{k}) = \frac{2 \langle S^z \rangle}{\exp(\beta E_k) - 1} \quad (135)$$

where  $\beta$  is  $1/k_B T$ .

By using the same technique that was used in Chap. IV to obtain Eq. (121), the following form is obtained for  $F(k)$  from Eq. (135) for temperatures above the Curie temperature.

$$F(\vec{k}) = \frac{\theta}{\gamma_o - \gamma_k + \chi^{-1}} \quad (M \rightarrow 0) \quad (136)$$

where the susceptibility,  $\chi$ , is given by Eq. (124). This is similar to the form used by Van Hove.<sup>40</sup> The most important implication of Eq. (136) is that at the Curie temperature where  $\chi^{-1}$  goes to zero,  $F(k)$  becomes very large for small values of  $|\vec{k}|$ , which in turn implies a large neutron cross-section for diffuse magnetic scattering at small angles.

The disappearance of the  $\langle S_{\text{o}}^z S_{\delta}^z \rangle$  correlation function above the Curie temperature seems to be a deficiency of the Green function technique used in this thesis since the symmetry of the Hamiltonian when the applied field is zero would lead one to expect that  $\langle S_{\text{o}}^z S_{\delta}^z \rangle = \langle S_{\text{o}}^x S_{\delta}^x \rangle = \langle S_{\text{o}}^y S_{\delta}^y \rangle = \langle S_{\text{o}}^+ S_{\delta}^- \rangle / 2$ .

## CHAPTER VII

### CONCLUSIONS

Because of the agreement between the results of these calculations, using equations derived by using H. B. Callen's termination procedure in the first order double-time temperature-dependent Green function equation and the termination function given by Eq. (40), and the results of other methods of calculation, it is believed that these results are good approximations to the physical behavior of the Heisenberg model over the whole temperature range. The comparison of these results and the behavior of nickel and iron indicates that the general magnetic behavior of these elements is explained by the basic Heisenberg model. It is hoped that the question of the temperature dependence of the effective magnetic moment of nickel and iron will be resolved by further neutron diffraction experiments.



## APPENDICES

# APPENDIX I

## COMPUTER PROGRAM

The computer program, which is written in Algol 60 for the Burroughs' B-5500 computer, calculates the sums  $\Phi_0$  and  $\Phi_\delta$  as functions of R, Eq. (95). The parameter R is convenient for calculation because it eliminates the need for reiteration.

Once  $\Phi_0$  and  $\Phi_\delta$  have been calculated for a value of R and a type of lattice, it is a matter of algebra to calculate the corresponding temperature and magnetization for any value of spin, S, by using Eqs. (40), (50), (51c), (57), (79), (89), and (94) which can be summarized using the program notation,  $C = \Phi_0$  and  $D = \Phi_\delta$

$$M = \frac{(S - C)(1 + C)^{2S+1} + (S + 1 + C)C^{2S+1}}{S[(1 + C)^{2S+1} - C^{2S+1}]} \quad (140)$$

$$T = R(2SM + M^4 D) \quad (141)$$

For  $S = 1/2$  the energy divided by  $NJ\gamma_0 S^2$  is given by

$$E = M^2 + 4MD + 4M^5 D^2 \quad (142)$$

The values of C and D ( $\Phi(0)$  and  $\Phi(D)$ ) computed for a set of values of R are tabulated in Appendix II.

The running time of the program is reduced by a factor of about 15 from the time it would take to sum over all the points in  $k$ -space for a certain lattice by taking advantage of the equivalence of many points. For this calculation the point  $(k_x, k_y, k_z)$  is equivalent to seven other points generated by changing the signs of  $k_x$ ,  $k_y$ , and  $k_z$ . By making the restraint that the lattice have equal size in the X and Y directions, it is convenient to also include in the same set the points generated by interchanging the values of  $k_x$  and  $k_y$ . The maximum number of points in a set,  $U$ , is  $2^4$  or 16. If  $k_x = k_y$ ,  $k_x = 0$  or  $\pi$ ,  $k_y = 0$  or  $\pi$ ,  $k_z = 0$  or  $\pi$ , then  $U$  is reduced by one power of 2 for each relation that is true since  $+0 = -0$  and  $+\pi$  and  $-\pi$  are equivalent because of the  $2\pi$  periodicity. One and only one point of each set is summed over by restricting the sum to the following volume of  $k$ -space:  $(0 \leq X \leq W/2, X \leq Y \leq W/2, 0 \leq Z \leq H/2)$  where  $\vec{k} = 2\pi(X/W, Y/W, Z/H)$ ,  $X$ ,  $Y$ , and  $Z$  are integers,  $W$  is the size of the lattice in the X and Y directions, and  $H$  is the size of the lattice in the  $Z$  direction. The values of  $H$  and  $W$  must be even in this program.

The space summed over is  $1/16$  of  $k$ -space. Another way of determining the value of  $U$  for each point is as follows. The points which are entirely within the subspace are weighted by a factor,  $U$ , of 16 in the sum. The points which lie on the boundary of the subspace are weighted by 16 multiplied by the fraction of the immediate surrounding volume which is in the subspace. For example a point on the interior of

one of the faces of the subspace would be at the center of a small sphere that was half in the subspace and would be weighted by  $U = 8$ . The points on the edges and corners of the subspace are weighted by factors of  $U = 4, 2$ , or  $1$  depending on their exact location. The weighting factor,  $U$ , appears in the sums  $C$  (for  $\Phi_0$ ) and  $D$  (for  $\Phi_\delta$ ) in procedure PR2. The program section with  $U = 3$  accounts for two sets such as  $(0, W/2, 0)$ ,  $U = 2$ , and  $(0, 0, H/2)$ ,  $U = 1$ .

The first run over the points in  $k$ -space is to evaluate the cosine and sine functions that are independent of  $R$  and store the values in arrays EB, EN, NN, and NB. This is accomplished by procedure PR1.

Next  $R$  is set to its initial value and  $\Phi_0$  and  $\Phi_\delta$  are calculated by running over the points in  $k$ -space and using procedure PR2. The last part of the program evaluates algebraic expressions for temperature, magnetization, and energy for the current value of  $R$  and prints out the results. Then the program control returns to the "FOR  $R$ " statement which sets  $R$  equal to the next listed value and repeats the operations described in this paragraph.

The program can be used on the Burroughs' B-5500 to find sums for up to 10 values of  $R$  for  $H = W = 40$  within 10 minutes. A face-centered-cubic lattice of this size with  $S = 1/2$  has a Curie point of  $\theta_c = 4.53$  which is 1.6 per cent higher than the bulk  $\theta_c$  which is 4.46. The results for very large  $H$  and  $W$  can be approximated better by letting each point represent a cubic cell in  $k$ -space centered around the

point whose width is equal to the distance between points,  $d$ . Instead of evaluating the summand,  $f$ , at the point, the average value over the cell is approximated by expanding  $f$  about the point in a Taylor series. The zero order term will be  $f$  evaluated at the center point which gives the same result as before. The first order terms are of the form  $f^x(X_o) \cdot (X - X_o)$  which has an average value of zero over the range of  $X$ ,  $(X_o - d/2, X_o + d/2)$ , where  $X_o$  is the center point and the superscript indicates a partial derivative. The second order terms of the form  $(1/2) f^{xx}(X_o) \cdot (X - X_o)^2$  are the only terms of second or third order which have a non-zero average value over the cell. The average value of these terms for a point or cell,  $\vec{k}$ , is

$$g(\vec{k}) = (f^{xx}(\vec{k}) + f^{yy}(\vec{k}) + f^{zz}(\vec{k}))(d^2/24)$$

To approximate the bulk solution,  $H = W \rightarrow \infty$ , the same points are summed over as before, but the summand is changed from  $f(\vec{k})$  to  $f(\vec{k}) + g(\vec{k})$ . This technique using  $H = W = 30$  gives a value of  $\theta_c$  which is within 0.1 per cent of the bulk value.

The program which follows is a photographic reproduction of the computer print out. The procedures PR1 and PR2 shown are for a face-centered-cubic lattice. The modifications for simple-cubic and body-centered-cubic lattice calculations are shown separately after the entire program.

The computer program used to calculate the function  $\lambda(2\chi^{-1})$  defined by Eq. (120) is shown in this appendix as "Susceptibility Program." In this program the integral equation

$$\frac{1}{2\pi} \int_{-\pi}^{\pi} \frac{dz}{a + b \cos(z)} = \frac{1}{(a^2 - b^2)^{1/2}}$$

has been used to reduce the three dimensional integral involved in Eq. (120) to a two dimensional integral which is evaluated by the computer. A region near the origin has been reduced to a one dimensional integral by making the approximations  $\cos(x) = 1 - x^2/2$  and  $\cos(y) = 1 - y^2/2$ . The error in the values of  $\lambda(2\chi^{-1})$  calculated by this program is 0.1 per cent or less. The results are shown in Tables 7 and 8 in Appendix II.

```

      BEGIN
FILE OUT      LINE 4 (2,15)}

FORMAT OUT    HEAD (X45,"FACE-CENTERED-CUBIC"/X23,"*",X7,"ALL SPIN",
               X10,"*      SPIN 1/2",X8,"*      SPIN 7/2  *"/X23,
               " R      PHI(0)      PHI(n)      KT/J      MAG.  ENERGY",
               "      KT/J      MAG."/) ;

FORMAT OUT    RESULT (X20,F6.1,2E11.3,F9.3,2F7.3,F10.3,F7.3) ;

REAL          A,B,C,D,E,F,G,H,J,K,L,M,N,O,P,Q,R,S,T,U,V,W,X,Y,Z,HC,HH,
               PI,M1,T1,CX,CY,CZ,SX,SY,SZ
INTEGER       I,I2
REAL ARRAY    EB,EN,NN,NB(0:30,0:1000) ;
PROCEDURE     PR1) BEGIN I+I+1 ;
               IF I>1000 THEN BEGIN I+0 ; I2+I2+1 END ;
               CX+COS(PI*X/W) ; CY+COS(PI*Y/W) ; CZ+COS(PI*Z/W) ;
               SX+SIN(PI*X/W) ; SY+SIN(PI*Y/W) ; SZ+SIN(PI*Z/W) ;
               EN(I2,I)+CX*CY+CY*CZ+CZ*CX ;
               EB(I2,I)+CX*CY-CY*CZ-CZ*CX ;
               NN(I2,I)+16*(SX*2*(CY+CZ)*2+SY*2*(CX+CZ)*2+
                                   SZ*2*(CX+CY)*2) ;
               NB(I2,I)+16*(SX*2*(CY-CZ)*2+SY*2*(CX-CZ)*2+
                                   SZ*2*(CX+CY)*2) ;
               END ;
PROCEDURE     PR2) BEGIN I+I+1 ;
               IF I>1000 THEN BEGIN I+0 ; I2+I2+1 END ;
               N+1/(EXP(A*B*EN(I2,I)+HH)-1) ;
               G+1/(EXP(A*B*EB(I2,I)+HH)-1) ;
               N+N*(1+(NN(I2,I)*(2*N*2+3*N+1)/R*2-( 8*EN(I2,I))*(N+1)/R)*P) ;

```

```

G+G*(1+(NB[I2,I]*(2*N+2+3*N+1)/R+2-( 8*EB[I2,I]*(N+1)/R)*P))
C+C+(N+3*G)*U )
D+D+(N*EN[I2,I]+G*EB[I2,I]*3)*U )
END )

H+30 ) W+30 )
PI+3.1415926 )
P+(P/W)*2/24 )
WRITE (LINE,HEAD) )
BEGIN
FOR X+2 STEP 1 UNTIL (W/2-1) DO
FOR Y+1 STEP 1 UNTIL ( X-1) DO
FOR Z+1 STEP 1 UNTIL (H/2-1) DO
PR1 )
FOR X+1 STEP 1 UNTIL (W/2-1) DO
FOR Y+0,X DO
FOR Z+1 STEP 1 UNTIL (H/2-1) DO
PR1 )
X+W/2 )
FOR Y+1 STEP 1 UNTIL (W/2-1) DO
FOR Z+1 STEP 1 UNTIL (H/2-1) DO
PR1 )
FOR X+2 STEP 1 UNTIL (W/2-1) DO
FOR Y+1 STEP 1 UNTIL (X-1) DO
FOR Z+0,H/2 DO
PR1 )
FOR X+1 STEP 1 UNTIL (W/2-1) DO
BEGIN Y+X)
FOR Z+0,H/2 DO
PR1 END )
X+0) Y+W/2) FOR Z+1 STEP 1 UNTIL (H/2-1) DO
PR1 )
FOR X+W/2,0 DO

```



```

      BEGIN Y+X ;
      FOR Z+1 STEP 1 UNTIL (H/2-1) DO
      PR1 END ;
      FOR X+1 STEP 1 UNTIL (W/2-1) DO
      FOR Y+0,W/2 DO
      FOR Z+0,H/2 DO
      PR1 ;
      X+W/2 ; FOR Y+0,W/2 DO BEGIN Z+0 ;
      PR1 END ;
      X+Y+W/2 ; Z+H/2 ;
      PR1 ;
      X+Y+0 ; Z+0,AA ;
      PR1 ;
      HC+0 ; COMMENT FOR ZERO APPLIED FIELD ;
      FOR R+0.2 STEP 0.2 UNTIL 2.01,2.5 STEP 0.5 UNTIL 9.5,
      10 STEP 1 UNTIL 20,24,30,40,60,100,200,500,1000,2000 DO
      BEGIN
      A+12/R ; B+4/R ; COMMENT FACE-CENTERED-CUBIC ONLY ;
      I+12+0 ;
      U+16 ;
      FOR X+2 STEP 1 UNTIL (W/2-1) DO
      FOR Y+1 STEP 1 UNTIL ( X-1) DO
      FOR Z+1 STEP 1 UNTIL (H/2-1) DO
      PR2 ;
      U+ 8 ;
      FOR X+1 STEP 1 UNTIL (W/2-1) DO
      FOR Y+0,X DO
      FOR Z+1 STEP 1 UNTIL (H/2-1) DO
      PR2 ;
      U+ 8 ;
      X+W/2 ;
      FOR Y+1 STEP 1 UNTIL (W/2-1) DO

```

```

FOR Z+1 STEP 1 UNTIL (H/2-1) DO
PR2 ;
U+ 8 ;
FOR X+2 STEP 1 UNTIL (W/2-1) DO
FOR Y+1 STEP 1 UNTIL (X-1) DO
FOR Z+0,H/2 DO
PR2 ;
U+ 4 ;
FOR X+1 STEP 1 UNTIL (W/2-1) DO
BEGIN Y+X;
FOR Z+0,H/2 DO
PR2 END ;
U+ 4 ;
X+0; Y+W/2; FOR Z+1 STEP 1 UNTIL (H/2-1) DO
PR2 ;
U+ 2 ;
FOR X+W/2,0 DO
BEGIN Y+X ;
FOR Z+1 STEP 1 UNTIL (H/2-1) DO
PR2 END ;
U+ 4 ;
FOR X+1 STEP 1 UNTIL (W/2-1) DO
FOR Y+0,W/2 DO
FOR Z+0,H/2 DO
PR2 ;
U+ 3 ;
X+W/2 ; FOR Y+0,W/2 DO BEGIN Z+0 ;
PR2 END ;
U+ 1 ; PR2 ; PR2 ;
C+C/(4*H*W*2) ; D+D/(12*H*W*2) ; COMMENT F.C.C. ONLY ;
COMMENT M,T,E FOR S=1/2, M1,T1 FOR S=7/2 ;
M+1/(1+2*C) ;

```

```

T+R*(M+2*M*4*D) )
E+M*2+4*M*D+4*M*5*D*2 )
M1+((3.5-C)*(1+C)*8+(4.5+C)*C*8)/((1+C)*8-C*8)*2/7 )
T1+R*(7*M1+2*M1*4*D) )
WRITE (LINE,RESULT,R,C,D,T,M,E,T1,M1) )
HH*0.0003417*HC/T ) COMMENT FOR NICKEL,S=1/2, HC IS FIELD KOE )
I+I2+C*D*0 )
END END END .

```

Computer Program, Sheet 5

Procedures:

```

COMMENT BODY-CENTERED-CUBIC ;
PROCEDURE PR1; BEGIN I+I+1 ;
      IF I>1000 THEN BEGIN I+0 ; I2+I2+1 END ;
      CX+COS(PI*X/W) ; CY+COS(PI*Y/W) ; CZ+COS(PI*Z/H) ;
      SX+SIN(PI*X/W) ; SY+SIN(PI*Y/W) ; SZ+SIN(PI*Z/H) ;
      EN[I2,I]+CX*CY*CZ ;
      EB[I2,I]+EN[I2,I] ;
      NN[I2,I]+64*((SX*CY*CZ)*2+(CX*SY*CZ)*2+(CX*CY*SZ)*2) ;
      NB[I2,I]+NN[I2,I] ;
      END ;
PROCEDURE PR2; BEGIN I+I+1 ;
      IF I>1000 THEN BEGIN I+0 ; I2+I2+1 END ;
      N+1/(EXP(A-B*EN[I2,I]+HH)-1) ;
      G+1/(EXP(A-B*EB[I2,I]+HH)-1) ;
      N+N*(1+(NN[I2,I]*(2*N+2+3*N+1)/R+2-( 24*EN[I2,I])*(N+1)/R)*P) ;
      G+G*(1+(NB[I2,I]*(2*N+2+3*N+1)/R+2-( 24*EB[I2,I])*(N+1)/R)*P) ;
      C+C+(N+ G)*U ;
      D+D+(N*EN[I2,I]+G*EB[I2,I])*U ;
      END ;

```

Line 77:

```

A+B/R ; R+B/R ; COMMENT BODY-CENTERED-CUBIC ONLY ;

```

Line 121:

```

C+C/(2*H*W*2) ; D+D/( 2*H*W*2) ;

```

Computer Program Modifications for Body-centered-cubic Lattice

## Procedures:

```

COMMENT SIMPLE CUBIC ;
PROCEDURE PR1; BEGIN I:=I+1 ;
      IF I>1000 THEN BEGIN I:=0 ; I2:=I2+1 END ;
      EN(I2,I):= COS(2*PI*X/W)+COS(2*PI*Y/W)+COS(2*PI*Z/W) ;
      VN(I2,I):=4*(SIN(2*PI*X/W)*2+SIN(2*PI*Y/W)*2+SIN(2*PI*Z/W)
                                     *2) ;
      END ;
PROCEDURE PR2; BEGIN I:=I+1 ;
      IF I>1000 THEN BEGIN I:=0 ; I2:=I2+1 END ;
      N:=1/(EXP(A=R*EN(I2,I)+HR)-1) ;
      N:=N*(1+(NN(I2,I)*(2*N+2+3*N+1)/R+2-( 2*EN(I2,I))*(N+1)/R)*P)) ;
      C:=C+N*I ;
      D:=D+ N*EN(I2,I)*U ;
      END ;

```

Line 77:

```

      A:=A/R ; R:=R/R ; COMMENT SIMPLE CUBIC ONLY ;

```

Line 121:

```

      C:=C/( H*W*2) ; D:=D/(3* H*W*2) ;

```

```

      BEGIN
FILE OUT      LINE 4 (2,15);

FORMAT      HEAD (X25,"FACE-CENTERED-CUBIC"//

              X19,"INV.SUS.      LAMBDA      3KT/4JS(S+1)      "///

FORMAT      RESULT (F25.4,2F12.3) ;

REAL      A,B,C,D,E,F,G,H,J,K,L,M,N,O,P,Q,R,S,T,U,V,W,X,Y,Z,HC,HH,
              PI,M1,T1,CX,CY,CZ,SX,SY,SZ ;
INTEGER      I,I2 ;
REAL ARRAY  EB,EN,NN,NB(0:30,0:1000) ;
PROCEDURE  PR1; BEGIN I+I+1 ;
              IF I>1000 THEN BEGIN I+0 ; I2+I2+1 END ;
              CX+CUS(PI*X/W) ; CY+CNS(PI*Y/W) ;
              EN(I2,I)+4*(CX*CY) ;
              NN(I2,I)+4*(CX+CY) ;
              NB(I2,I)+4*(CX-CY) ;
              END ;
PROCEDURE  PR2; BEGIN I+I+1 ;
              IF I>1000 THEN BEGIN I+0 ; I2+I2+1 END ;
              C+C+U/SQRT((I2+2*S-EN(I2,I))+2-NN(I2,I)+2) +
              U/SQRT((I2+2*S+EN(I2,I))+2-NB(I2,I)+2) ;
              END ;
              N+200 ;
              PI+3.1415926 ;
              WRITE (LINE,HEAD) ;

      BEGIN

```

```

FOR X=2 STEP 1 UNTIL (W/2-1) DO
FOR Y=1 STEP 1 UNTIL (X-1) DO
PR1 ;
FOR X=2 STEP 1 UNTIL (W/2-1) DO
FOR Y=0,X DO
PR1 ;
X=W/2 ;
FOR Y=1 STEP 1 UNTIL (W/2-1) DO
PR1 ;
X=0 ; Y=W/2 ;
PR1 ;
X=Y+W/2 ;
PR1 ;
FOR S=0.0000001,0.0005,0.0007,0.001,0.0015,0.002,0.003,0.005,
0.007,0.01,0.015,0.02,0.03,0.05,0.07,0.1,0.15,0.2,0.3,
0.5,0.7,1,1.5,2,3,5,7,10,15,20,30,50,100 DO
BEGIN
I=I2+0 ;
U=5 ;
FOR X=2 STEP 1 UNTIL (W/2-1) DO
FOR Y=1 STEP 1 UNTIL (X-1) DO
PR2 ;
U=4 ;
FOR X=2 STEP 1 UNTIL (W/2-1) DO
FOR Y=0,X DO
PR2 ;
X=W/2 ;
FOR Y=1 STEP 1 UNTIL (W/2-1) DO
PR2 ;
U=2 ;

```

```

X+0 ; Y+W/2 ;
PR2 ;
U+1 ;
X+Y+W/2 ;
PR2 ;
FOR Z+0.150 STEP 0.150 UNTIL 1.45 DO
D+D+2*Z/SQRT((PI*XZ/W)*2+S/2) ;
FOR Z+0.075 STEP 0.150 UNTIL 1.45 DO
D+D+4*Z/SQRT((PI*XZ/W)*2+S/2) ;
Z+0.15 ;
D+D+ Z/SQRT((PI*XZ/W)*2+S/2) ;
C+C+9*(PI/1440*D+(4-PI)/32/SQRT((1.80*PI/W)*2+S/2)) ;
L+(12+2*S)*C/(2*W*2) ;
I+(6+S)/L ;
M+M1 ; M1+LN(T*4.461962) ;
Q+T1 ; T1+LN(S) ;
E+(Q-T1)/(M-M1) ; IF S<0.0001 THEN E+0 ;
WRITE (LINE,RESULT,S,L,T) ;
I+I2+C+D+0 ;
END END END .

```

Susceptibility Program, Sheet 3



## APPENDIX II

### COMPUTER RESULTS

This appendix contains tables of results obtained by using the basic program and modifications described in Appendix I.

Tables 4, 5, and 6 list the sums  $\Phi_0$  and  $\Phi_\delta$  defined by Eq. (95) for a set of values of  $R$ . The three tables are for the three types of cubic lattices, face-centered, body-centered, and simple. The values of the reduced temperature,  $k_B T/J$ , the relative magnetization,  $M$ , and the fraction of the magnetic exchange energy,  $E$ , as calculated from Eqs. (140), (141), and (142) for  $S = 1/2$  are listed for each value of  $R$ . Also values of  $k_B T/J$  and  $M$  for another value of  $S$  are listed.

Tables 6 and 7 list the values of inverse susceptibility,  $\chi^{-1}$ , defined by Eq. (122), the function  $\lambda(2\chi^{-1})$  defined by Eq. (120) (under LAMBDA), and the reduced temperature  $\theta = 3k_B T/4JS(S+1)$  corresponding to the value of  $\chi^{-1}$  as given by Eq. (124). Table 6 is for a face-centered-cubic lattice and Table 7 is for a body-centered-cubic lattice.

The notation  $1.357 @-03$  represents  $1.357 \times 10^{-3}$ .

## FACE-CENTERED-CUBIC

★ ALL SPIN ★			★ SPIN 1/2 ★			★ SPIN 7/2 ★	
R	PHI(0)	PHI(D)	KT/J	MAG.	ENERGY	KT/J	MAG.
0.2	1.318E-03	1.300E-03	0.200	0.997	1.000	1.400	1.000
0.4	3.772E-03	3.668E-03	0.400	0.993	1.000	2.800	0.999
0.6	7.010E-03	6.718E-03	0.599	0.986	0.999	4.200	0.998
0.8	1.092E-02	1.030E-02	0.798	0.979	0.998	5.599	0.997
1.0	1.546E-02	1.434E-02	0.995	0.970	0.997	6.997	0.996
1.2	2.060E-02	1.877E-02	1.191	0.960	0.996	8.395	0.994
1.4	2.635E-02	2.353E-02	1.384	0.950	0.993	9.790	0.992
1.6	3.273E-02	2.857E-02	1.573	0.939	0.991	11.183	0.991
1.8	3.977E-02	3.386E-02	1.757	0.926	0.987	12.573	0.989
2.0	4.750E-02	3.935E-02	1.936	0.913	0.982	13.959	0.986
2.5	6.995E-02	5.372E-02	2.352	0.877	0.964	17.398	0.980
3.0	9.643E-02	6.846E-02	2.716	0.838	0.940	20.787	0.972
3.5	1.278E-01	8.385E-02	3.024	0.796	0.910	24.111	0.963
4.0	1.624E-01	9.914E-02	3.277	0.755	0.879	27.356	0.954
4.5	2.001E-01	1.144E-01	3.482	0.714	0.847	30.513	0.943
5.0	2.403E-01	1.297E-01	3.647	0.675	0.816	33.572	0.931
5.5	2.827E-01	1.448E-01	3.779	0.639	0.787	36.528	0.919
6.0	3.269E-01	1.599E-01	3.885	0.605	0.761	39.376	0.907
6.5	3.725E-01	1.750E-01	3.970	0.573	0.737	42.112	0.894
7.0	4.193E-01	1.899E-01	4.040	0.544	0.716	44.733	0.880
7.5	4.672E-01	2.048E-01	4.096	0.517	0.697	47.238	0.867
8.0	5.160E-01	2.197E-01	4.143	0.492	0.680	49.628	0.853
8.5	5.655E-01	2.345E-01	4.182	0.469	0.665	51.901	0.839
9.0	6.157E-01	2.493E-01	4.214	0.448	0.652	54.060	0.825
9.5	6.665E-01	2.640E-01	4.241	0.429	0.640	56.107	0.811
10.0	7.177E-01	2.787E-01	4.265	0.411	0.630	58.045	0.797
11.0	8.214E-01	3.040E-01	4.301	0.378	0.612	61.604	0.769
12.0	9.263E-01	3.372E-01	4.329	0.351	0.598	64.770	0.742
13.0	1.032E+00	3.663E-01	4.350	0.326	0.587	67.577	0.715
14.0	1.139E+00	3.954E-01	4.366	0.305	0.577	70.062	0.689
15.0	1.247E+00	4.244E-01	4.379	0.286	0.569	72.259	0.665
16.0	1.355E+00	4.534E-01	4.390	0.270	0.563	74.203	0.641
17.0	1.463E+00	4.823E-01	4.399	0.255	0.557	75.924	0.618
18.0	1.572E+00	5.112E-01	4.406	0.241	0.553	77.449	0.596
19.0	1.681E+00	5.401E-01	4.412	0.229	0.548	78.804	0.576
20.0	1.791E+00	5.690E-01	4.417	0.218	0.545	80.010	0.556
24.0	2.231E+00	6.842E-01	4.431	0.183	0.535	83.686	0.487
30.0	2.895E+00	8.568E-01	4.442	0.147	0.527	87.010	0.408
40.0	4.008E+00	1.144E+00	4.451	0.111	0.520	89.809	0.317
60.0	6.241E+00	1.718E+00	4.457	0.074	0.515	91.924	0.218
100.0	1.072E+01	2.864E+00	4.459	0.045	0.513	93.043	0.133
200.0	2.192E+01	5.729E+00	4.461	0.022	0.512	93.522	0.067
500.0	5.554E+01	1.432E+01	4.461	0.009	0.511	93.657	0.027
1000.0	1.116E+02	2.865E+01	4.461	0.004	0.511	93.676	0.013
2000.0	2.237E+02	5.730E+01	4.461	0.002	0.511	93.680	0.007

Table 4. Computer Results for  $\phi_0$  and  $\phi_\delta$  for a Face-centered-cubic Lattice

## BODY-CENTERED-CUBIC

★ ALL SPIN ★			★ SPIN 1/2 ★			★ SPIN 1 ★	
R	PHI(0)	PHI(D)	KT/J	MAG.	ENERGY	KT/J	MAG.
0.1	9.281E-04	9.178E-04	0.100	0.998	1.000	0.200	0.999
0.2	2.650E-03	2.594E-03	0.200	0.995	1.000	0.400	0.997
0.3	4.911E-03	4.757E-03	0.300	0.990	1.000	0.600	0.995
0.4	7.628E-03	7.307E-03	0.399	0.985	0.999	0.800	0.992
0.5	1.076E-02	1.019E-02	0.499	0.979	0.999	0.999	0.989
0.6	1.428E-02	1.335E-02	0.598	0.972	0.998	1.198	0.986
0.7	1.817E-02	1.677E-02	0.696	0.965	0.997	1.396	0.982
0.8	2.244E-02	2.043E-02	0.793	0.957	0.995	1.594	0.978
0.9	2.709E-02	2.429E-02	0.889	0.949	0.994	1.791	0.973
1.0	3.214E-02	2.833E-02	0.984	0.940	0.992	1.986	0.968
1.2	4.346E-02	3.691E-02	1.167	0.920	0.986	2.370	0.957
1.6	7.127E-02	5.553E-02	1.505	0.875	0.967	3.107	0.930
2.0	1.058E-01	7.539E-02	1.790	0.825	0.939	3.782	0.897
2.4	1.464E-01	9.588E-02	2.021	0.773	0.905	4.379	0.860
2.8	1.920E-01	1.166E-01	2.201	0.723	0.870	4.891	0.821
3.2	2.417E-01	1.375E-01	2.339	0.674	0.836	5.323	0.781
3.6	2.945E-01	1.583E-01	2.444	0.629	0.804	5.681	0.741
4.0	3.500E-01	1.790E-01	2.524	0.588	0.776	5.976	0.703
4.4	4.075E-01	1.997E-01	2.586	0.551	0.752	6.219	0.667
4.8	4.667E-01	2.202E-01	2.634	0.517	0.730	6.418	0.633
5.2	5.273E-01	2.407E-01	2.671	0.487	0.712	6.583	0.601
5.6	5.890E-01	2.611E-01	2.701	0.459	0.696	6.719	0.572
6.0	6.516E-01	2.814E-01	2.725	0.434	0.682	6.833	0.545
6.4	7.150E-01	3.017E-01	2.744	0.412	0.670	6.929	0.519
6.8	7.791E-01	3.218E-01	2.760	0.391	0.660	7.009	0.496
7.2	8.438E-01	3.420E-01	2.773	0.372	0.651	7.078	0.474
7.9	9.581E-01	3.771E-01	2.791	0.343	0.638	7.175	0.440
8.6	1.074E+00	4.121E-01	2.805	0.318	0.627	7.250	0.410
9.3	1.190E+00	4.470E-01	2.815	0.296	0.618	7.309	0.383
10.0	1.307E+00	4.819E-01	2.823	0.277	0.611	7.356	0.360
10.7	1.425E+00	5.166E-01	2.830	0.260	0.606	7.394	0.339
11.4	1.543E+00	5.513E-01	2.835	0.245	0.601	7.426	0.320
12.1	1.662E+00	5.860E-01	2.839	0.231	0.597	7.452	0.303
12.8	1.781E+00	6.206E-01	2.843	0.219	0.593	7.474	0.288
13.5	1.900E+00	6.552E-01	2.846	0.208	0.590	7.492	0.274
14.2	2.020E+00	6.897E-01	2.848	0.198	0.587	7.508	0.261
16.0	2.328E+00	7.785E-01	2.853	0.177	0.582	7.540	0.233
20.0	3.016E+00	9.753E-01	2.860	0.142	0.575	7.582	0.188
30.0	4.747E+00	1.466E+00	2.866	0.095	0.568	7.623	0.127
50.0	8.222E+00	2.446E+00	2.869	0.057	0.564	7.643	0.076
100.0	1.693E+01	4.894E+00	2.870	0.029	0.563	7.652	0.038
250.0	4.305E+01	1.224E+01	2.870	0.011	0.562	7.654	0.015
500.0	8.660E+01	2.447E+01	2.870	0.006	0.562	7.654	0.008
1000.0	1.737E+02	4.895E+01	2.870	0.003	0.562	7.654	0.004

Table 5. Computer Results for  $\phi_0$  and  $\phi_\delta$  for a Body-centered-cubic Lattice

## SIMPLE CUBIC

★ ALL SPIN			★ SPIN 1/2			★ SPIN 7/2 ★	
R	PHI(0)	PHI(D)	KT/J	MAG.	ENERGY	KT/J	MAG.
0.1	1.860e-03	1.833e-03	0.100	0.996	1.000	0.700	0.999
0.2	5.327e-03	5.175e-03	0.200	0.989	1.000	1.400	0.998
0.3	9.905e-03	9.482e-03	0.299	0.981	0.999	2.100	0.997
0.4	1.544e-02	1.455e-02	0.398	0.970	0.998	2.799	0.996
0.5	2.187e-02	2.027e-02	0.496	0.958	0.997	3.498	0.994
0.6	2.918e-02	2.654e-02	0.592	0.945	0.995	4.196	0.992
0.7	3.736e-02	3.330e-02	0.686	0.930	0.993	4.892	0.989
0.8	4.642e-02	4.050e-02	0.777	0.915	0.990	5.587	0.987
0.9	5.634e-02	4.806e-02	0.865	0.899	0.986	6.280	0.984
1.0	6.712e-02	5.593e-02	0.949	0.882	0.981	6.969	0.981
1.2	9.116e-02	7.244e-02	1.104	0.846	0.970	8.338	0.974
1.5	1.329e-01	9.849e-02	1.300	0.790	0.947	10.354	0.962
1.8	1.805e-01	1.254e-01	1.454	0.735	0.922	12.315	0.948
2.1	2.329e-01	1.527e-01	1.572	0.682	0.896	14.209	0.933
2.4	2.892e-01	1.800e-01	1.660	0.634	0.871	16.024	0.917
2.7	3.485e-01	2.074e-01	1.726	0.589	0.848	17.755	0.900
3.0	4.104e-01	2.346e-01	1.776	0.549	0.828	19.395	0.883
3.3	4.742e-01	2.618e-01	1.813	0.513	0.811	20.942	0.865
3.6	5.397e-01	2.888e-01	1.842	0.481	0.795	22.394	0.846
3.9	6.065e-01	3.157e-01	1.865	0.452	0.782	23.750	0.828
4.2	6.744e-01	3.425e-01	1.883	0.426	0.771	25.013	0.809
4.5	7.433e-01	3.692e-01	1.897	0.402	0.761	26.185	0.790
4.8	8.129e-01	3.958e-01	1.908	0.381	0.753	27.268	0.771
5.1	8.831e-01	4.223e-01	1.917	0.362	0.746	28.269	0.753
5.4	9.539e-01	4.488e-01	1.925	0.344	0.740	29.191	0.735
6.0	1.097e+00	5.016e-01	1.936	0.313	0.729	30.819	0.699
6.5	1.217e+00	5.454e-01	1.944	0.291	0.722	31.980	0.671
7.0	1.338e+00	5.890e-01	1.949	0.272	0.717	32.988	0.644
7.5	1.460e+00	6.326e-01	1.953	0.255	0.712	33.864	0.619
8.0	1.582e+00	6.762e-01	1.957	0.240	0.708	34.626	0.594
8.5	1.705e+00	7.196e-01	1.960	0.227	0.705	35.290	0.571
9.0	1.828e+00	7.630e-01	1.962	0.215	0.703	35.871	0.550
9.5	1.952e+00	8.063e-01	1.964	0.204	0.700	36.380	0.529
10.0	2.076e+00	8.496e-01	1.965	0.194	0.698	36.829	0.510
10.5	2.200e+00	8.929e-01	1.967	0.185	0.697	37.225	0.492
11.0	2.324e+00	9.361e-01	1.968	0.177	0.695	37.575	0.474
12.0	2.573e+00	1.023e+00	1.970	0.163	0.693	38.165	0.443
15.0	3.322e+00	1.281e+00	1.973	0.131	0.688	39.335	0.368
20.0	4.577e+00	1.711e+00	1.976	0.098	0.684	40.290	0.285
30.0	7.095e+00	2.571e+00	1.978	0.066	0.681	40.993	0.194
50.0	1.214e+01	4.287e+00	1.979	0.040	0.680	41.360	0.118
100.0	2.477e+01	8.577e+00	1.979	0.020	0.679	41.515	0.059
250.0	6.265e+01	2.144e+01	1.979	0.008	0.679	41.559	0.024
500.0	1.258e+02	4.289e+01	1.979	0.004	0.679	41.565	0.012
1000.0	2.521e+02	8.578e+01	1.979	0.002	0.679	41.567	0.006

Table 6. Computer Results for  $\Phi_0$  and  $\Phi_D$  for a Simple-cubic Lattice

## FACE-CENTERED-CUBIC

INV.SUS.	LAMBDA	3KT/4JS(S+1)
0.0000	1.344	4.464
0.0005	1.337	4.489
0.0007	1.335	4.493
0.0010	1.334	4.499
0.0015	1.332	4.507
0.0020	1.330	4.514
0.0030	1.326	4.526
0.0050	1.321	4.545
0.0070	1.317	4.561
0.0100	1.312	4.581
0.0150	1.305	4.609
0.0200	1.299	4.633
0.0300	1.290	4.674
0.0500	1.276	4.743
0.0700	1.264	4.801
0.1000	1.251	4.878
0.1500	1.233	4.988
0.2000	1.219	5.087
0.3000	1.197	5.264
0.5000	1.166	5.574
0.7000	1.145	5.854
1.0000	1.121	6.243
1.5000	1.095	6.849
2.0000	1.078	7.424
3.0000	1.055	8.528
5.0000	1.033	10.648
7.0000	1.022	12.718
10.0000	1.014	15.781
15.0000	1.008	20.841
20.0000	1.005	25.874
30.0000	1.002	35.910
50.0000	1.001	55.940
100.0000	1.000	105.951

Table 7. Computer Results for Inverse Initial Susceptibility,  $\mu H/2SJM$ , for a Face-centered-cubic Lattice and the Function  $\lambda(2\chi^{-1})$

## BODY-CENTERED-CUBIC

INV.SUS.	LAMBDA	3KT/4JS(S+1)
0.0000	1.393	2.872
0.0005	1.383	2.893
0.0007	1.381	2.897
0.0010	1.379	2.902
0.0015	1.376	2.908
0.0020	1.373	2.914
0.0030	1.369	2.924
0.0050	1.362	2.940
0.0070	1.357	2.953
0.0100	1.350	2.970
0.0150	1.341	2.994
0.0200	1.334	3.014
0.0300	1.321	3.050
0.0500	1.303	3.109
0.0700	1.288	3.159
0.1000	1.271	3.226
0.1500	1.249	3.324
0.2000	1.231	3.412
0.3000	1.204	3.571
0.5000	1.168	3.854
0.7000	1.143	4.114
1.0000	1.116	4.479
1.5000	1.088	5.055
2.0000	1.070	5.608
3.0000	1.048	6.680
5.0000	1.027	8.763
7.0000	1.018	10.810
10.0000	1.011	13.852
15.0000	1.006	18.890
20.0000	1.004	23.911
30.0000	1.002	33.932
50.0000	1.001	53.943
100.0000	1.001	103.920

Table 8. Computer Results for Inverse Initial Susceptibility,  $\mu H/2SJM$ , for a Body-centered-cubic Lattice and the Function  $\lambda(2\chi^{-1})$

### APPENDIX III

#### RENORMALIZED ENERGIES

The renormalized energies are part of the concept in which the ground state,  $|0\rangle$ , of the Heisenberg ferromagnet serves as the background for the creation of quasiparticle spinwaves, or magnons. The magnons obey Bose statistics and exist in  $N$  energy levels corresponding to the  $N$  magnon (or spinwave) creation operators,  $S_k^-$ . The statistical expectation value of the number of particles in the energy level denoted by  $k$  at a temperature  $T$  is

$$n_k = \frac{1}{\exp(E_k^{sw}(T)/k_B T) - 1} \quad (150)$$

where  $E_k^{sw}(T)$  is the energy required to create a magnon in the particular level. The creation energy is temperature dependent because there is not only the energy necessary to create the magnon in the ground state,  $E_k^{sw}$  (corresponding to kinetic energy of a real particle), but there is an interaction energy,  $E_{k,k}^{sw}$ , with each magnon that is already present. The number of other magnons present in the various energy levels at temperature,  $T$ , is also given by Eq. (150). From Eq. (3b)

$$E_k^{sw} = 2SJ(\gamma_o - \gamma_k) \quad (151)$$

$$\gamma_k = \sum_{\delta} \exp(i\vec{k} \cdot \vec{\delta}) \quad (152)$$

where  $\delta$  represents the set of real space vectors from a lattice site to its nearest neighbors. The interaction energy is defined by

$$E_{k, k'} = \langle k, k' | \mathcal{H} | k, k' \rangle - \langle k' | \mathcal{H} | k' \rangle - \langle k | \mathcal{H} | k \rangle \quad (153)$$

If, in the spirit of the first order perturbation theory, the non-diagonal terms in the sum on the right side of Eq. (3e) are ignored, the Eqs. (153), (3b), and (3e) imply that

$$E_{k, k'} = -4SJN^{-1}(\gamma_o - \gamma_k + \gamma_{k'-k} - \gamma_{k'}) \quad (154)$$

By using Eqs. (150), (151), and (154) the renormalized creation energy for a magnon in energy level  $k$  is

$$E_k^{sw}(T) = E_k^{sw} + \sum_{k'} n_{k'} E_{k, k'} \quad (155)$$

This result agrees with the renormalized energies found by M. Bloch<sup>36</sup> from a technique of minimizing the free energy, and with the first



order results found by Dyson<sup>7</sup> from considering the Born scattering of two spinwaves. Because of the cubic symmetry requirements placed on  $n_{\mathbf{k}}$  and  $\gamma_{\mathbf{k}}$  by the lattice

$$\sum_{\mathbf{k}'} n_{\mathbf{k}'} (\gamma_{\mathbf{k}'-\mathbf{k}} - \gamma_{\mathbf{k}'}) = -(\gamma_0 - \gamma_{\mathbf{k}}) \gamma_0^{-1} \sum_{\mathbf{k}'} n_{\mathbf{k}'} \gamma_{\mathbf{k}'} \quad (156)$$

By using Eqs. (151), (154), and (156), Eq. (155) can be written

$$E_{\mathbf{k}}^{\text{sw}}(T) = 2SJ \left[ 2 \langle S^z \rangle + \frac{2}{N \gamma_0} \sum_{\mathbf{k}'} n_{\mathbf{k}'} \gamma_{\mathbf{k}'} \right] (\gamma_0 - \gamma_{\mathbf{k}}) \quad (157)$$

All of the spinwave energies are reduced by the factor in square brackets which is independent of  $\mathbf{k}$ . At low temperatures, only the lowest energy levels are appreciably occupied. To obtain the first order behavior of the renormalization factor, the following approximation is made for a simple cubic lattice

$$E_{\mathbf{k}}^{\text{sw}} = J(\gamma_0 - \gamma_{\mathbf{k}}) = J |\vec{\mathbf{k}}|^2 = Jk^2 \quad (158)$$

Using this approximation which produces spherical symmetry and replacing the sum by the equivalent integral

$$2 \langle S^z \rangle = 1 - \frac{2}{N} \sum_{\mathbf{k}} \frac{1}{\exp(k^2/\theta) - 1} \quad (159)$$

$$= 1 - c_1 \theta^{3/2}$$

$$c_1 = \frac{1}{\pi^2} \int_0^\infty \frac{x^2 dx}{\exp(x^2) - 1}$$

The second term in the renormalization factor becomes

$$\frac{-2}{N \gamma_0} \sum_{\mathbf{k}'} n_{\mathbf{k}'} \gamma_{\mathbf{k}'} = \frac{-1}{(2\pi)^3} \int_0^\infty \frac{(2 - k^2) 4\pi k^2 dk}{\exp(k^2/\theta) - 1} \quad (160)$$

$$= c_1 \theta^{3/2} - c_2' \theta^{5/2}$$

The approximation made in Eq. (158) suppresses some terms of order  $\theta^{5/2}$  and higher in Eqs. (159) and (160), however it can be seen that the lowest order temperature term in the expansion for  $\langle S^z \rangle$  is  $\theta^{3/2}$  and the lowest order term for the renormalization factor is  $\theta^{5/2}$ .

While the Green function technique is not tied to a quasiparticle concept, it can be shown that for a system of true Bose particles, the poles of the Green function correspond to the creation or excitation energies. The commutator of the creation and destruction operators for Bose particles is necessarily unity, however for the magnons

$$\left[ S_k^+, S_k^- \right] = 2 \langle S^z \rangle \quad (161)$$

which differs from unity at low temperatures by a term of order  $\theta^{3/2}$ . It might be expected that the energies of spinwave theory would agree with the poles from the Green function to first order at low temperatures.

The poles of the Green functions are given by Eq. (48). Using Eq. (50) and letting  $H' = 0$

$$E_k = J \left[ 2 \langle S^z \rangle + \frac{4\alpha \langle S^z \rangle}{N} \sum_{k'} \frac{\exp(ik' \cdot \delta)}{\exp(E_{k'}/k_B T) - 1} \right] (\gamma_0 - \gamma_k) \quad (162)$$

The sum is independent of the particular nearest vector,  $\delta$ , used so  $\exp(ik \cdot \delta)$  can be replaced by  $\gamma_k / \gamma_0$ . If the low temperature limit of  $\alpha$  is  $1/2S$ , then the poles of the Green function,  $E_k$ , in the low temperature limit do agree with renormalized spinwave energies, Eq. (157), up to order  $\theta^{5/2}$ .

## BIBLIOGRAPHY

BIBLIOGRAPHY<sup>\*</sup>

1. P. Weiss, J. de Phys. 6, 667 (1907).
2. J. H. Van Vleck, Rev. Mod. Phys. 17, 27 (1945).
3. W. Heisenberg, Zeits fur Physik 49, 619 (1928).
4. P. A. M. Dirac, The Principles of Quantum Mechanics (Oxford Univ. Press, N. Y.) (1935), second edition, Chap. X.
5. C. Kittel, Introduction to Solid State Physics (John Wiley & Sons, N. Y., 1963), p. 112.
6. F. Bloch, Z. Physik 61, 206 (1930); 74, 295 (1932).
7. F. J. Dyson, Phs. Rev. 102, 1217 and 1230 (1956).
8. P. R. Weiss and J. H. Van Vleck, Phys. Rev. 55, 673 (1939) and P. R. Weiss, doctor's thesis, Harvard Univ. (1941).
9. J. S. Kouvel and M. E. Fisher, Phys. Rev. 136, A1626 (1964).
10. W. Opechowski, Physica 4, 181 (1937).
11. C. Domb and M. F. Sykes, Phys. Rev. 128, 168 (1962).
12. Noakes and Arrott, J. Appl. Phys. 35, 931 (1964).
13. N. N. Bogolyubov and S. V. Tyablikov, Doklady Akad. Nauk. 126, 53 (1959) Translation: Soviet Phys. - Doklady 4, 589 (1959).
14. S. V. Tyablikov, Ukr. Math. Zhur. 11, 287 (1959).
15. D. N. Zubarev, Soviet Phys. - USPEKHI 3, 320 (1960).
16. M. Wortis, Phys. Rev. 132, 85 (1963).
17. T. Tanaka and T. Morita, Bull. Am. Phys. Soc. 9, 463 (1964).
18. I. Ortenburger, Phys. Rev. 136, A1374 (1964).

19. H. B. Callen, Phys. Rev. 130, 890 (1963).
20. D. J. Thouless, The Quantum Mechanics of the Many-Body Systems (Academic Press, N. Y., 1961), Chap. 5.
21. N. N. Bogolyubov and O. S. Parasyuk, Dokl. Akad. Nauk. SSSR 109, 717 (1956).
22. R. A. Tahir-Kheli and D. ter Haar, Phys. Rev. 127, 88 (1962).
23. P. Weiss and R. Forrer, Ann. Phys. 5, 153 (1926).
24. H. A. Brown and J. M. Luttinger, Phys. Rev. 100, 686 (1955).
25. B. Widom and O. K. Rice, J. Chem. Phys. 23, 1250 (1955).
26. J. Smit and H. P. J. Wijn, Ferrites (John Wiley and Sons, N. Y.) (1959), p. 9.
27. C. G. Shull and Y. Yamada, J. Phys. Soc. Japan 17 B-III, 1 (1962).
28. R. E. Marburger, Phys. Rev. Letters 8, 487 (1962).
29. R. Gersdorf, Phys. Rev. Letters 10, 155 (1963).
30. F. Menzinger and A. Paoletti, Phys. Rev. Letters 10, 290 (1963).
31. S. Arajas, J. Appl. Phys. 36, 1136 (1965).
32. S. J. Glass and M. J. Klein, Phys. Rev. 109, 288 (1958).
33. R. M. Bozorth, Ferromagnetism (D. Van Nostrand, N. Y.) (1963), p. 736.
34. G. N. Watson, Quart. J. Math. 10, 266 (1939).
35. M. Tikson, J. Res. Natl. Bur. Std. 50, 177 (1953).
36. M. Bloch, Phys. Rev. Letters 9, 286 (1962).
37. K. P. Belov, Magnetic Transitions (Consultants Bureau, N. Y.) (1961), p. 58.

38. R. D. Lowde, J. Appl. Phys. 36, 884 (1965).
39. T. Riste, J. Phy. Soc. Japan 17, 60 (1962).
40. L. Van Hove, Phys. Rev. 95, 1374 (1954).
41. H. A. Gersch, C. G. Shull, M. K. Wilkinson, Phys. Rev. 103, 525 (1956).
42. B. T. Matthias, R. M. Bozorth, and J. H. Van Vleck, Phys. Rev. Letters 7, 160 (1961).

\*Standard abbreviations used are from the American Institute of Physics Style Manual (1962).

## VITA

John Alexander Copeland, III was born February 6, 1941 in Atlanta, Georgia. He lived in Atlanta with his parents, Mr. and Mrs. John A. Copeland, Jr., attending public elementary schools and Northside and Westminster high schools until entering the School of Physics at the Georgia Institute of Technology in September 1958. On June 22, 1960, Sandra Jean Chandler became his wife. He completed the requirements for a B.S. degree in Physics in September 1961 and received a M.S. degree in Physics in June 1963.

He worked as an engineer at radio stations WAKE and WLAW during the summer and fall of 1958. Since 1959 he has worked for the Engineering Experiment Station at Georgia Tech where since 1961 he has been supervisor of the Solid State Electronics Laboratory, a group doing research on the physical properties of thin metallic and insulating films. He worked during the summer of 1961 as an Associate Scientist at the Jet Propulsion Laboratories in Pasadena, California.

He is a member of Lambda Chi Alpha social fraternity, and Sigma Pi Sigma, Pi Mu Epsilon, Tau Beta Pi, Phi Kappa Phi, and Phi Eta Sigma honor societies.